International Journal of Energy and Power Engineering
2024, Vol. 13, No. 6, pp. 108-134
https://doi.org/10.11648/j.ijepe.20241306.11

Research Article

General Concept of the Magnetic Reconnection Converter (MRC)

Oleg Agamalov*

Electrical Department, Tashlyk pump-storage power plant, Pivdennoukrainsk, Ukraine

Abstract

The general concept of the magnetic reconnection converter (MRC) is considered, based on the cyclic combination of two physical processes: 1) controlled turbulence using super-linear Richardson diffusion and/or self-generated/self-sustaining physical processes increases the stochasticity of the magnetic field (MF) in a limited volume of plasma and, accordingly, the global helicity H through the processes of twisting, writhing, and linking of the MF flow tubes to the level of a local maximum (optimally global), which is determined by the plasma parameters, boundary conditions, magnetic tension of the field lines, etc. At this stage of the MF turbulent pumping, the β of plasma will decrease to the minimum possible value with a corresponding increasing in the accumulated "topological" MF energy; 2) upon reaching the local (if possible global) maximum of MF stochasticity, turbulent magnetic reconnection (TMR) occurs in the plasma, which reduces the state of the local (if possible global) maximum of MF stochasticity and increases the kinetic stochasticity of plasma particles, accelerating and heating them, which is used in direct converters of electrical power. At this stage of turbulent discharge, the β of plasma will increasing to the maximum possible value with a corresponding increasing in its kinetic and thermal energy; 3) when the kinetic stochasticity of plasma particles subsequently decreases and reaches a local minimum, the control system repeats the MF turbulent pumping in the plasma and the cycles are repeated. Practically, the basis of the MRC can be the fusion scheme of two anti-spiral spheromaks, the helicity of which is increased in a cycle with the help of controlled turbulence before their fusion and the creation of a field-reversed configuration (FRC) to increase the efficiency of the annihilation of their toroidal and poloidal magnetic fields into kinetic and thermal energy of plasma particles with its subsequent direct transformation into electrical power for industrial use or single-volume plasma (spheromak) with changing beta at turbulent pumping/discharge phases of the working cycle.

Keywords

Controlled Turbulence, Magnetic Stochasticity, Magnetic Reconnection, Kinetic Stochasticity, Spheromaks, Field-Reversed Configuration

1. Introduction

Magnetic reconnection (MR) is a fundamental process by which magnetic fields in conductive mediums topologically rearrange themselves due to breaking the frozen state and moving to a lower energy state releasing stored magnetic energy [1-5]. The magnetic energy released by reconnection is transformed into kinetic, thermal, and non-thermal energy of plasma's particles [6-10]. MR is a multi-scale physical phenomenon that preserves the magnetic topology on the

*Corresponding author: olegagamalov@gmail.com (Oleg Agamalov)

Received: 1 November 2024; **Accepted:** 19 November 2024; **Published:** 29 November 2024

macro scale, constraining a plasma evolution at disturbances so that stresses build up free energy in the form of current sheets (CS). At the micro-scale appears a violation of the frozen state and magnetic flux slip relative to the motions of the plasma due to different nonidealities effects in plasma (e.g., turbulence, resistivity, finite gyroradius effects, etc), and a destabilization of CSs in plasma. This micro-scale topological redistribution releases built-up magnetic energy as plasma heating, bulk outflows, particle acceleration, shock waves, and other effects of kinetic stochasticity. The region where the topological rearrangement occurs is the reconnection region or diffusion region (DR) [2-4].

The topology of magnetic fields is determined through a generalizing parameter – global magnetic helicity H, which determines the degree of tangling or braiding of their lines and flux tubes and has 3 main components: 1) twisting, 2) linking, and 3) writhing [11]:

$$H = \int_V u \cdot \omega d\, V = \sum_{i \neq j} \Gamma_i \Gamma_j K_{ij} + \sum_i \Gamma_i^2 \left(T_{wi} + W_{ri}\right) \quad (1)$$

where the integral is performed over all space where exists magnetofluid with a magnetic field (MF), and each index labels a vortex tube of magnetic flux Γ_i (u, ω are velocity and vorticity of this magnetic flux, and dV a volume element), and the first term of right side (1) is mutual helicity due linking i-j flux tubes (or lines) with factor K_{ij}, and the second term of right side (1) is self-helicity due twisting with factor Twi and writhing with factor W_{ri}. Magnetic helicity is practically constant with the ideal moving of the medium (continuous deformations of flow tubes). Twisting T_{wi} is a changeable local parameter while linking K_{ij} and writhing W_{ri} are non-local parameters of MF flux tubes (lines). At stretching flux tubes (lines) of a MF, writhing can turn into twisting. At compressing flux tubes (lines) of a MF, it is vice versa. Magnetic helicity is constant H = const if resistivity of medium η = 0. Twisted flux ropes store free magnetic energy, which may be released either in individual flux ropes in the nonlinear phase of the ideal kink instability, or through interaction of multiple twisted flux ropes [3]. In the former case, the field relaxes to a state of minimum magnetic energy through internal magnetic reconnections as well as reconnection with ambient untwisted field lines. In the latter case, multiple flux ropes reduce their energy through reconnecting into a single flux rope. For two flux ropes, the energy release is found to be substantially greater if the flux ropes initially have opposite currents (twisted in reverse senses) than if the currents are in the same direction [2-4]. This is because the former configuration has zero helicity, and hence the relaxed state has lower energy. However, the opposite-twisted flux ropes are much less likely to relax and release the free energy, since neither the toroidal or poloidal magnetic field components reverse at the interface between the flux ropes, and there is no obvious way - apart perhaps from a strong external perturbation - in which magnetic reconnection could be initiated. Next, we will consider that for the proposed magnetic reconnection converter (MRC), as a strong external disturbance, we will use the physical process of turbulent pumping through a super-linear Richardson cascade and/or self-generated/self-sustaining turbulence.

There are three basic particle acceleration processes at MR: 1) Fermi acceleration which takes place as particles stream along, and drift in relaxing curved MF lines and due reflection in plasmoids, 2) relatively localized electric fields $E_{||}$ parallel to the MF, directly accelerate particles, and 3) betatron heating which occurs as particles drift into regions of stronger MF while conserving the first adiabatic moment $\mu = \frac{mv_{\perp}^2}{B}$ [12]:

$$\frac{d\varepsilon}{dt} = qE_{||}v_{||} + \mu\frac{dB}{dt} + qE \cdot u_c + \frac{1}{2}m\frac{d}{dt}|u_E|^2 \quad (2)$$

where ε is the energy of a MR output particle, u_E is the E ×B drift velocity, $\frac{d}{dt} = \frac{\partial}{\partial t} + u_E \cdot \nabla$, $E_{||}$ is the parallel electric field, and $v_{||}$ is the drift-corrected guiding center parallel velocity. For slowly varying fields, u_c is the curvature drift of particles and reduces to $u_c \sim \frac{mv_{||}^2}{qB}$(b×k), where k = b·∇b is the magnetic field curvature and b is the unit vector in the direction of the magnetic field. The terms on the right-hand side (2) represent correspondently energy gain by the parallel electric field, betatron heating, Fermi acceleration, and the polarization drift respectively, and the first three mechanisms are sketched in Figure 1 [12]:

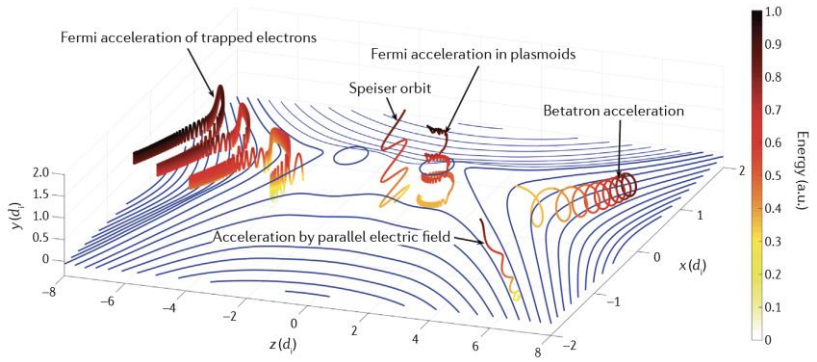

Figure 1. *Illustration of MR particle acceleration mechanisms.*

As shows on figure 1 MR in a localized diffusion region connects together oppositely directed magnetic fields to create new, more bended magnetic field lines with strong magnetic tension that are ejected at the Alfven velocity to form outflow plasma jets and causing the inflow of upstream plasma and magnetic flux so that process is a self-maintaining [7]. In a real magnetized fluid (plasma), the magnetic diffusivity (resistivity) η and viscosity ν may be small but finite or ν, $\eta \to 0$ ($\neq 0$), and as a result exist turbulence (as in astrophysical and laboratory systems) [13-15], and ideal MHD cannot be applied. In [16] present a mathematical formalism of a scale-split energy density, $\psi_{l,}=B_l \cdot B_L/2$ for vector field B(x, t) renormalized at scales l and L to quantify the notion of the field topological deformation, topology change, and magnetic stochasticity level. For MF it is shown that the evolution of the field topology is directly related to the field-fluid slippage at MR. The velocity field at the turbulence can be approached similarly to a kinetic stochasticity level. Then MR, which can occur on a wide range of scales as a result of nonlinearities at large scales (turbulence inertial range) and nonidealities at small scales (dissipative range), is a relaxation process by which the MF lowers both its topological entanglements induced by turbulence and its energy level. When MF decreases its magnetic stochasticity induced by the turbulent flow by slipping through the fluid, it may accelerate magnetized fluid (plasma) particles.

In general, MR may be considered as a physical process that transforms magnetic stochasticity into kinetic stochasticity [17-21]. And vice versa, kinetic stochasticity may be effectively increased through super-linear Richardson diffusion in turbulent cascades [5, 17, 24] and by using feedback, when MR creates turbulence as a self-generated and/or self-sustaining physical process [5, 10, 22, 23]. In this paper we proposed a general concept of the magnetic reconnection converter (MRC), that is based on the cyclic combination of these two physical processes: 1) controlled turbulence using super-linear Richardson diffusion and/or by self-generated/self-sustaining physical process increases the stochasticity of MF in a limited volume of plasma and, accordingly, the global helicity H through the processes of twisting, writhing, and linking of the MF flow tubes to the level of a local maximum (optimally global), which is determined by the plasma parameters, boundary conditions, magnetic tension of the field lines, etc. At this stage of the MF turbulent pumping, the β of plasma will decrease to the minimum possible value with a corresponding increase in the accumulated "topological" energy of the MF; 2) upon reaching the local (if possible global) maximum of MF stochasticity, turbulent magnetic reconnection (TMR) occurs in the plasma, which reduces the state of the local (if possible global) maximum of MF stochasticity and increases the kinetic stochasticity of plasma particles, accelerating and heating them, which is used in direct converters of electrical power and outer coils of electromagnetic inductions (explanation follows). At this stage of turbulent discharge, the β of plasma will be increasing to the maximum possible value with a corresponding increase in its kinetic and thermal energy; 3) when the kinetic stochasticity of plasma particles subsequently decreases and reaches a local minimum, the control system repeats the MF turbulent pumping in the plasma and the cycles are repeated. Practically, the basis of the MRC can be realized as the fusion scheme of two counter-helicity spheromaks, the helicity of which is increased in a cycle with the help of controlled turbulence before their fusion and the creation of a field-reversed configuration (FRC) to increase the efficiency of the transformation (annihilation) of their toroidal and poloidal magnetic fields into kinetic and thermal energy of plasma particles with its subsequent direct transformation into electrical power for industrial use. So, we use counter-helicity turbulent magnetic reconnection (CHTMR). However, in our opinion, the MRC framework is more perspective-based, based on single-volume plasma with changing β at turbulent pumping/discharge phases of the working cycle.

As for the structure of this paper, our goal is to present the theoretical possibility of the MRC's general concept with controlled turbulence-driven reconnection. In Section 2 we consider the relationship between topological complexity, helicity, and MF energy. The framework and work cycle of MRC is substantiated in Section 3. Section 4 presents the possibility of MRC realization based on a fusion of counter-helicity spheromaks (SPHs) with pre-executed turbulence pumping and as a single-volume plasma with various beta (relation plasma pressure to magnetic pressure) in the work cycle, and estimation of their efficiency. We provide a summary and discussion in Section 5. Finally, the calculation of early considered MRC realization and their efficiency in the PYTHON code is presented in the Appendixes A-E.

2. The Relationship Between Topological Complexity, Helicity, and Magnetic Field Energy

First, we consider a limited volume of plasma with a boundary area and a MF and describe the increase of the MF energy in the plasma due to the increase of helicity (as a parameter corresponding to topological complexity and magnetic stochasticity) under the influence of turbulent pumping using super-linear Richardson diffusion or self-driven, self-sustained turbulence. Let's define the following basic parameters, concepts and assumptions:

Magnetic Helicity H: for a measure of the magnetic stochasticity through twisting, linking and writhing of MF flux tubes.

Turbulent Pumping P: the transfer of energy from small-scale turbulent motions (eddies) to large-scale MF.

Richardson's Super-linear Diffusion or self-driven, self-sustained turbulence T: an enhanced diffusion process in turbulent plasmas where the diffusion coefficient increases with the scale size of the turbulent eddies.

Plasma Volume V: The volume of plasma under consideration.

Boundary Area S: The surface area enclosing the plasma volume.

Magnetic Field B: The magnetic field within the plasma volume.

The evolution of magnetic helicity in a plasma volume is governed by the helicity balance equation:

$$\frac{dH}{dt} = 2\int_V E \cdot B dV - \int_S (E \times B + \nabla\psi) dS + \frac{\partial H}{\partial t}\Big]_P \quad (3)$$

where: (dH/dt) is rate of change of magnetic helicity within the volume, E is electric field (EF), B is MF, ψ is helicity flux function, $\partial H/\partial t|_P$ is rate of change of helicity due to turbulent pumping. The increase in MF energy is related to the helicity injection rate through:

$$\frac{\partial\left(\frac{B^2}{2\mu_0}\right)}{\partial t} = \frac{\mu_0}{V}\frac{\partial H}{\partial t} \quad (4)$$

where μ_0 is the permeability of free space. The turbulent pumping term ($\partial H/\partial t|_P$) can be modeled using Richardson's super-linear diffusion (we assume that this component also includes mechanisms of self-generated and self-sustained turbulence):

$$\frac{\partial H}{\partial t}\Big]_P = \nabla \cdot (D\nabla H) \quad (5)$$

where D is the turbulent diffusion coefficient, which depends on the scale size of the turbulent eddies and can be expressed as $D = D_0 (l/l_0)^{\alpha}$ with D_0 as the reference diffusion coefficient, l is the scale size of turbulent eddies, l_0 is reference scale size, and α is Super-linear diffusion exponent (typically $\alpha > 1$).

The mathematical model (3)-(5) describes the increase in magnetic field energy due to helicity injection under the influence of turbulent pumping driven by Richardson's super-linear diffusion and includes mechanisms of self-generated and self-sustained turbulence. Key points of this system are:

The model captures the interplay between magnetic helicity, turbulent pumping, and super-linear diffusion in driving magnetic field amplification.

The turbulent diffusion coefficient D plays a crucial role in determining the efficiency of energy transfer from small-scale turbulence to large-scale magnetic fields.

The model can be extended to include other physical processes, such as magnetic reconnection and dynamo action, to provide a more comprehensive description of magnetic field evolution in turbulent plasmas.

Solving this system of equations requires knowledge of the electric field E, the helicity flux function ψ, and the turbulent eddy scale size l, which may be obtained from experimental measurements or numerical simulations of the plasma.

This system of equations, along with appropriate boundary conditions and initial conditions, can be solved numerically to study the dynamics of magnetic field amplification in turbulent plasmas.

Relative to this model turbulent pumping of MF energy through increasing helicity appears to be an interesting question: if the energy of the magnetic field is proportional to $B^2/2\ \mu_0$, i.e. only to the square of the magnitude of the induction vector, and helicity does not affect it, why can a more complex topology of the magnetic field correspond to a greater field energy? However, a more complex magnetic field topology can indeed lead to a higher overall magnetic energy within a given volume V, and here's why:

Increased field strength in localized regions: a complex MF topology often involves regions of higher field strength due to twisting, linking, and writhing of the MF lines. A more complex magnetic field topology often requires more field lines and/or stronger field gradients to maintain its structure. This translates to a higher overall magnetic field strength B in certain regions, leading to an increase in the total magnetic energy within the plasma volume, even though the energy density itself is still just $B^2/2\mu_0$. In some cases, a complex topology might also lead to the formation of current sheets or other localized regions of high current density, which can further contribute to the magnetic energy. Even if the average field strength remains the same, these localized regions of higher B contribute disproportionately to the total magnetic energy due to the square dependence.

Increased volume of the MF: a more complex topology might lead to the MF occupying a larger effective volume. Think of a tangled flux tube taking up more space than a straight one. This increased volume, even with the same average field strength, results in a higher total magnetic energy.

Helicity and energy dynamics: while helicity H doesn't directly appear in the magnetic energy formula, it plays a crucial role in the dynamics and evolution of the MF. Higher helicity H often implies a more complex and tangled field configuration. Processes that increase helicity, like turbulent pumping or dynamo action, can lead to the generation of stronger magnetic fields and thus higher magnetic energy.

We can refine the formula of magnetic field energy within a volume V, $W = (1/2\mu_0) \int B^2\ dV$, to reflect the influence of topology or helicity H through their indirect effects on the magnetic field energy:

1. Incorporating Current Density:

The magnetic field energy can also be expressed in terms of the current density J using the vector potential A:

$$W = (1/2) \int (J \cdot A)\ dV,$$

This formulation highlights the contribution of currents to

the MF energy. Complex topologies often involve higher current densities, leading to increased energy.

2. Helicity-Based Correction:

While a direct analytical relationship between helicity and energy is complex, we can introduce a phenomenological correction factor to account for the stabilizing effect of helicity $W = (1/2\mu_0) \int B^2 dV * f(H)$,

where f(H) is a function that increases with helicity (H), reflecting the tendency of higher helicity configurations to support stronger magnetic fields and currents.

3. Topology-Dependent Term:

In principle, we could introduce a term that explicitly depends on the topological complexity of the magnetic field. However, defining and quantifying such complexity is challenging. One possible approach is to use the magnetic field line length (L) as a proxy for topological complexity: $W = (1/2\mu_0) \int B^2 dV + g(L)$,

where g(L) is a function that increases with the total length of magnetic field lines within the volume, capturing the additional energy associated with more convoluted topologies.

Caveats and Considerations:

The refined formulas with helicity or topology-dependent terms are more conceptual than rigorously derived.

The exact functional forms of f(H) and g(L) would depend on the specific plasma configuration and require further theoretical or empirical investigation.

Numerical simulations can provide valuable insights into the relationship between topology, helicity, and magnetic field energy in various plasma systems.

Therefore, while the simplified magnetic energy formula doesn't directly include topology or helicity, we can refine it to capture their indirect effects. These refinements highlight the contributions of current density, helicity-induced stability, and topological complexity to the overall magnetic field energy within a given volume. Further exploration into advanced theoretical models and numerical simulations is necessary to fully understand the intricate relationship between topology, helicity, and magnetic energy in complex plasma configurations, and it may be theme of further explorations.

3. The Framework and Work Cycle of MRC

In [5, 13-21, 25] considered turbulent magnetic reconnection (TMR). At fast TMR, turbulent mixing of plasma parcel trajectories with MF flux tubes appears in a turbulent inertial range (on any inner scale). If we define the unit tangent vector on l-scale, $\hat{B}_l = B_l/B_l$ then in this scale the components of the coarse-grained induction equation are:

$$\partial_t \hat{B}_l = \frac{\nabla\times(u_l\times B_l)^{\perp}}{B_l} - (\Sigma_l^{\perp} + \sigma_l^{\perp}),\ \partial_t B_l = \nabla\times(u_l\times B_l)^{\parallel} - B_l\left(\Sigma_l^{\parallel} + \sigma_l^{\parallel}\right) \quad (6)$$

where $(.)^{\perp}$ indicates the perpendicular component to the l-scale field B_l that defines MF topology changing, $(.)^{(\parallel)}$ indicates the parallel component to the l-scale field B_l that defines MF energy changing, u_l is plasma parcel velocity in the l-scale. Parameters connected with slipping "field-plasma" in turbulent and laminar modes are:

$$\Sigma_l = \frac{(\nabla\times R_l)}{B_l}, \sigma_l = \frac{(\nabla\times P_l)}{B_l},\ R_l = -(u\times B)_l + u_l\times B_l, P_l = E_l + (u\times B)_l \quad (7)$$

In (7) the term Σ_l governs MR in turbulence due to the non-linear term R_l (the turbulent electromotive force (EMF) $_l \equiv -R_l$, is the motional electric field induced by turbulent eddies of scales smaller than l), and σ_l to govern MR in laminar plasma parcels flows at l-scale due to the renormalized Ohm's law $P_l = E_l + (u\times B)_l$ or non-ideal effects in plasma on small scales. In [25] have shown, that the rate of magnetic topology change (MR rate) depends on the functional derivative of $B_l\Sigma_l$ (and $B_l\sigma_l$ on small scales in laminar flows):

$$\tau_T^{-1} \doteq \left|\sum_{k=1}^{3}\iiint d^3x \frac{\delta\left(B_l\Sigma_l^k\right)}{\delta B_l^k(x)}\right| \backsim \frac{\Delta u_l}{l} \quad (8)$$

(6)-(8) shows that magnetic topology changes on all turbulent inertial scales l in the turbulent inertial range, it is independent of small scale (non-ideal) effects in plasma, and is proportional to eddy turn-over rate on scale l. In laminar flows, this rate is proportional to negligible resistivity.

For general estimation of turbulence influence on MF topology and energy $\psi_{l,L}(x, t)$ in plasma in [16-21] defined the spatial complexity, or stochasticity level by $\mathcal{L}_p$-norm of the magnetic $S_p(t)$ and velocity $s_p(t)$ fields in an arbitrary spatial volume V on the coarse-grained scales l and L, and if take for simplicity p=2 we obtain the rms values:

$$\psi_{l,L}(x,t) = \frac{1}{2}B_lB_L, S_2(t) = \frac{1}{2}\left\|\hat{B}_l\hat{B}_L - 1\right\|_{rms}, s_2(t) = \frac{1}{2}\|\hat{u}_l\hat{u}_L - 1\|_{rms} \quad (9)$$

In general, turbulence in plasma tends to tangle and complicate initially smooth MF flux tubes increasing their entropy through the magnetic stochasticity level $\partial_t S_p \geq 0$. As these tangling and complicating increase, magnetic tension

forces of flux tubes will also increase, and at some point, this resistance can provide a sharp slippage of flux tubes in plasma or MR. At this point, $\partial_t S_p = 0$ and further magnetic stochasticity will be decreasing $\partial t S_p \leq 0$. If we define the derivative of magnetic stochasticity T_2 (p=2) then the phenomenon of MR will appear at the next conditions of MF [18]:

$$T_2(t) = \partial_t S_2(t) = \frac{1}{2}\partial_t\left(\left\|\hat{\boldsymbol{B}}_l\hat{\boldsymbol{B}}_L - 1\right\|_{rms}\right) = 0 \qquad \& \qquad \partial_t T_2(t) = \frac{1}{2}\partial_t^2\left(\left\|\hat{\boldsymbol{B}}_l\hat{\boldsymbol{B}}_L - 1\right\|_{rms}\right) < 0 \tag{10}$$

After meeting the conditions (10), and due to the action of magnetic tension which does not allow further increase of magnetic stochasticity $S_2(t)$, there is a sharp increase in kinetic stochasticity level to some maximal level, depending on the previously achieved level of magnetic stochasticity, that corresponds to plasma jets (particle acceleration):

$$\tau_2(t) = \partial_t s_2(t) = \frac{1}{2}\partial_t(\|\hat{u}_l\hat{u}_L - 1\|_{rms}) > 0 \qquad \& \qquad s_2(t) = \frac{1}{2}\|\hat{u}_l\hat{u}_L - 1\|_{rms} \to s_{2max}(t) \tag{11}$$

Condition (11) relaxing MF to some minimal magnetic stochasticity level depends on the achieved maximal level of kinetic stochasticity $s_{2max}(t)$.

Based on the equations system (3)-(11) we proposed the framework of the magnetic reconnection converter (MRC), which is based on the cyclic combination of these two physical processes: 1) controlled turbulence using super-linear Richardson diffusion and/or by self-generated/self-sustaining physical process increases the stochasticity of MF in a limited volume of plasma and, accordingly, the global helicity H through the processes of twisting, writhing, and linking of the MF flow tubes to the level of a local maximum (optimally global), which is determined by the plasma parameters, boundary conditions, magnetic tension of the field lines, etc accordingly equation (7). At this stage of the MF turbulent pumping, the β of plasma will decrease to the minimum possible value with a corresponding increase in the accumulated "topological" energy of the MF; 2) upon reaching the local (if possible global) maximum of MF stochasticity, turbulent magnetic reconnection (TMR) occurs in the plasma, which reduces the state of the local (if possible global) maximum of MF stochasticity and increases the kinetic stochasticity of plasma particles, accelerating and heating them accordingly equation (8), which is used in direct converters of electrical power and outer coils of electromagnetic inductions (explanation follows). At this stage of turbulent discharge, the β of plasma will be increasing to the maximum possible value with a corresponding increase in its kinetic and thermal energy; 3) when the kinetic stochasticity of plasma particles subsequently decreases and reaches a local minimum (after passing the maximum), the control system repeats the MF turbulent pumping in the plasma and the working cycles are repeated. In general, there is an analogy that the working cycle of the MRC uses the "breathing" of the plasma at different stages, namely "inhalation-exhalation" corresponds to the expansion-compression of the plasma in the volume.

Consider the general formal mathematical model of MRC. Let's delve into how the concept of turbulence-reconnection correlation can be incorporated into the specific formulas describing super-linear Richardson diffusion or self-generation/self-sustained turbulence mechanisms. In super-linear Richardson diffusion, the diffusion coefficient D increases faster than linearly with the scale size l. This leads to enhanced mixing and transport of magnetic field lines, potentially facilitating faster reconnection. The diffusion coefficient D in the helicity and energy evolution equations can be modified to include a dependence on the turbulent parameters. One possible approach is to express D as a function of the turbulent velocity fluctuations u', magnetic field fluctuations B', and the scale size l:

$$D = D_0\left(\frac{l}{l_0}\right)^{\alpha}\left(\frac{u'}{u_0}\right)^{\beta}\left(\frac{B'}{B_0}\right)^{\gamma} \tag{12}$$

where: D_0 is the reference diffusion coefficient, l_0, u_0, B_0 are reference scale size, velocity, and magnetic field, α, β, γ are exponents representing the scaling of diffusion with scale size, velocity fluctuations, and magnetic field fluctuations, respectively. For super-linear diffusion, $\alpha > 1$. The enhanced diffusion due to turbulence can lead to a faster dissipation of magnetic energy and a more efficient reconnection process. For generated and/or sustained turbulence by the reconnection process we must create a feedback loop where reconnection drives turbulence, which in turn enhances the reconnection rate. A source term representing the generation of turbulence due to reconnection can be added to the turbulence evolution equation. This term could depend on the reconnection rate, current density, or other relevant parameters. The enhanced turbulence can then be incorporated into the diffusion coefficient or the reconnection rate scaling, as described above, creating a feedback loop between reconnection and turbulence. The specific form of the modified diffusion coefficient or turbulence generation term will depend on the specific turbulence model and the physical mechanisms driving the turbulence-reconnection correlation. Numerical simulations play a crucial role in exploring the impact of these modifications on the reconnection dynamics and energy conversion process. Experimental validation is essential to compare the simulation results with real-world observations and refine the models further.

Let's formulate a general mathematical model in the form of a system of equations and inequalities that describes the

operation of a Magnetic Reconnection Converter (MRC) based on the combination of controlled turbulence and magnetic reconnection processes:

The controlled phase of turbulent pumping, which includes the following physical processes:

a. Helicity evolution:

$$\frac{dH}{dt} = 2\int_V E \cdot B dV - 2\eta \int_V (J \cdot B) dV + \alpha R_i I + f(\Gamma) \quad (13)$$

b. Magnetic energy evolution:

$$\frac{dW_{mag}}{dt} = -\int_S S \cdot dA - \eta \int_V J^2 dV + \beta \frac{dH}{dt} \quad (14)$$

c. β plasma decrease due magnetic energy increasing:

$$\frac{d\beta(t)}{dt} < 0 \quad (15)$$

d. Turbulent intensity increase:

$$\frac{dI}{dt} > 0 \quad (16)$$

f. Termination condition:

$$S_2(t) \geq S_{2minmax}(t) \quad \text{OR} \quad \beta(t) \leq \beta_{min} \quad (17)$$

The controlled phase of magnetic reconnection, which includes the following physical processes:

a. Energy Conversion:

$$\frac{dW_{mag}}{dt} = -\frac{dW_{kin}}{dt} - \frac{dW_{th}}{dt} - \eta \int_V J^2 dV \quad (18)$$

b. β plasma increase due magnetic energy decreasing:

$$\frac{d\beta(t)}{dt} > 0 \quad (19)$$

c. Kinetic stochasticity (particles acceleration) increase:

$$\frac{ds_2(t)}{dt} > 0 \quad (20)$$

d. Termination condition:

$$s_2(t) \geq s_{2minmax}(t) \quad \text{OR} \quad \beta(t) \geq \beta_{max} \quad (21)$$

Cycle Repetition

a. Kinetic Stochasticity Decrease:

$$\frac{ds_2(t)}{dt} < 0 \quad (22)$$

b. Termination condition:

$$s_2(t) \leq s_{2maxmin}(t) \quad \text{OR} \quad \beta(t) \geq \beta_{maxmin} \quad (23)$$

were, we use the following notations: f(Γ) represents the contribution from self-generation/self-sustained turbulence mechanisms, H is global magnetic helicity, B is magnetic field, β is plasma beta (ratio of plasma pressure to magnetic pressure), R_i is Richardson number, I is turbulence intensity, $S_2(t)$ is magnetic stochasticity, Γ is turbulence generation rate, W_{mag} is magnetic energy, W_{kin} is kinetic energy of plasma particles, W_{th} is thermal energy of plasma particles, η is magnetic diffusivity, E is electric field, and J is current density.

The efficiency of the MRC can be calculated as the ratio of the useful kinetic energy generated to the total energy input during the turbulent pumping stage. It may be achieved with use a sophisticated control system which to monitor the plasma parameters, initiate the different stages at the appropriate times, and optimize the overall efficiency of the MRC. This mathematical model provides a framework for describing the operation of an MRC based on controlled turbulence and magnetic reconnection. In ideal conditions, a significant portion of the magnetic energy injected during the turbulent pumping stage could be converted into kinetic energy of plasma particles during reconnection. Further research, numerical simulations, and experimental validation are necessary to refine the model, optimize the MRC design, and realize its potential for efficient energy conversion. The optimal plasma parameters, turbulence sources, and geometric dimensions for achieving of need useful power will depend on the specific design and configuration of the MRC. However, some general considerations include:

Plasma Parameters:

High plasma density and temperature to maximize the energy density and reconnection rate. Typical densities may be in the range of 10^{19} to 10^{21} particles per cubic meter. The plasma temperature should be sufficient to facilitate the desired turbulence and reconnection processes. Temperatures in the range of several million degrees Celsius are often required (a range of several keV (kilo-electron volts) might be required).

Low collisionality to facilitate efficient turbulent reconnection.

Appropriate magnetic field configuration to enable controlled turbulence and efficient reconnection. A strong magnetic field is necessary to confine the plasma and enable efficient energy conversion. Magnetic field strengths of several Tesla are typically used in fusion devices.

Turbulence Sources:

External injection of turbulence using electromagnetic waves, neutral beams or radio frequency heating.

Self-generation of turbulence through instabilities or dynamo action within the plasma. The plasma may self-organize into turbulent states under certain conditions, providing a potential source of turbulence for the MRC.

Geometric Dimensions:

The size and shape of the MRC will depend on the desired power output and the specific plasma parameters.

Optimization of the dimensions is crucial to ensure efficient energy conversion and minimize losses.

Challenges and Losses:

Energy Losses: Energy can be lost due to radiation, particle escape, viscosity, and other dissipation mechanisms during both turbulent pumping and reconnection stages.

Incomplete Energy Conversion: Not all of the magnetic energy may be converted into kinetic energy. Some may remain as thermal energy or residual magnetic energy in the FRC.

Control and Synchronization: Maintaining precise control over the turbulence and reconnection processes and synchronizing them effectively can be challenging, leading to inefficiencies.

MRC basic elements should include a plasma chamber that contains the plasma and magnetic fields, a turbulence generation system that injects or induces turbulence in the plasma, magnetic field coils that generate and control the magnetic field configuration, an energy extraction system that converts the kinetic energy of plasma particles into electrical power, and a reconnection control system that need to control and trigger the magnetic reconnection process.

4. Two ways of practical MRC realization

4a. Based on the mathematical model of general MRC (13)-(23) we can define the mathematical model of MRC, which realized fusion of two counter-helicity spheromaks (SPHs) with early made turbulent pumping, integrate the concept of super-linear Richardson diffusion or self-generation/self-sustained turbulence.

Stage 1: Spheromak (j=1, 2) formation and turbulent pumping.

Helicity evolution:

$$\frac{dH_j}{dt} = 2\int_V E_j \cdot B_j dV_j - 2\eta \int_V \left(J_j \cdot B_j\right) dV_j + \alpha_j R_{ij}{}^{m_j} I_j + f_j(\Gamma_j), \tag{24}$$

where $m_j > 1$ represent the super-linear dependence on the Richardson number.

Energy evolution:

$$\frac{dW_j}{dt} = -\int_S \boldsymbol{S}_j \cdot d\boldsymbol{A}_j - \eta \int_V \boldsymbol{J}_j{}^2 dV_j + \beta_j \frac{dH_j}{dt} \tag{25}$$

Turbulence Control:

$$H_j = F(I_j) \to H_{jmax} \tag{26}$$

where I_j are controlled to achieve desired helicity levels.

Termination Condition:

$$H_j \geq H_{jtarget} \quad OR \quad W_j \geq W_{jtarget} \tag{27}$$

Stage 2: Merging and Reconnection.

Reconnection Rate:

$$\frac{dR}{dt} \propto V_A \left(\frac{1}{L}\right)^{\frac{\alpha_{ij}}{2}} f(R_{ij})(\Gamma_{ij}) \tag{28}$$

In (28) the reconnection rate now depends on the Richardson numbers and turbulence generation rates of both SPHs.

Energy Conversion:

$$\frac{dW_1}{dt} + \frac{dW_2}{dt} = -\frac{dW_{FRC}}{dt} - \frac{dW_{kin}}{dt} - \frac{dW_{th}}{dt} - \frac{dW_{rad}}{dt} - \frac{dW_{loss}}{dt} \tag{29}$$

Helicity Evolution during Reconnection:

$$\frac{dH_{FRC}}{dt} = \frac{dH_1}{dt} + \frac{dH_2}{dt} - \frac{dH_{loss}}{dt} \tag{30}$$

Termination Condition:

$$R \geq R_{target} \tag{31}$$

Stage 3: Energy Extraction and Plasma Relaxation.

Energy Extraction:

$$\frac{dW_{kin}}{dt} = -P_{out} - \frac{dW_{th}}{dt} - \frac{dW_{loss}}{dt} \tag{32}$$

Plasma Relaxation:

$$\frac{dT}{dt} < 0, \ \frac{d\beta}{dt} < 0, \qquad \frac{dH_{FRC}}{dt} < 0 \tag{33}$$

Termination Condition:

$$W_{kin} \leq W_{kin\ min} \tag{34}$$

Cycle Repetition: the control system monitors $W_{kin,}$ when condition (34) holds, the system initiates Stage 1 again.

Key changes equations system (24)-(34) are:

The helicity evolution equations now include the super-linear dependence on the Richardson number $R_{ij}{}^{mj}$ that reflects the enhanced diffusion and turbulence at larger scales in super-linear Richardson diffusion and inclusion of $f_j(\Gamma_j)$ accounts for the contribution of self-generation/self-sustained turbulence mechanisms to the reconnection rate.

The reconnection rate formula incorporates the Richardson numbers and turbulence generation rates of both spheromaks.

The specific forms of the functions $R_{ij}{}^{mj}$ and $f_j(\Gamma_j)$ will

depend on the detailed turbulence and reconnection models used. Numerical simulations are crucial to explore the parameter space and optimize the MRC design and operation.

MRC which realized fusion of two counter-helicity spheromaks (SPHs) consist of three main chambers:

Two spheromaks formation chambers (left and right).

A central merging/reconnection chamber.

These chambers are connected by conduits or channels that allow for the controlled transfer of the spheromaks. The entire system is enclosed within a vacuum vessel to maintain the necessary plasma conditions. Each chamber contains MF coils to generate and sustain the SPH configuration, turbulence injection system (e.g., neutral beam injectors, RF antennas) to induce and control turbulence, diagnostics to monitor plasma parameters (density, temperature, magnetic field, etc.). Merging/reconnection chamber is larger than the SPH formation chambers to accommodate the merging and reconnection process and contains MF coils to guide and control the merging of the SPHs, diagnostics to monitor the reconnection process and the FRC formation, energy extraction system (e.g., direct energy converters) to convert the kinetic energy of accelerated particles into electrical energy. A central control system monitors and controls the entire MRC operation, including turbulence injection in the SPH chambers, SPH transfer and merging, reconnection process, energy extraction, plasma diagnostics and feedback control. Auxiliary systems include vacuum pumps to maintain the vacuum environment, power supplies for the MF coils and other systems, cooling systems to manage the heat generated during operation, shielding to protect the surrounding environment from radiation. Key functional blocks of the MRC based on a fusion of counter-helicity SPHs with pre-executed turbulence pumping are illustrated in the diagram, figure 2:

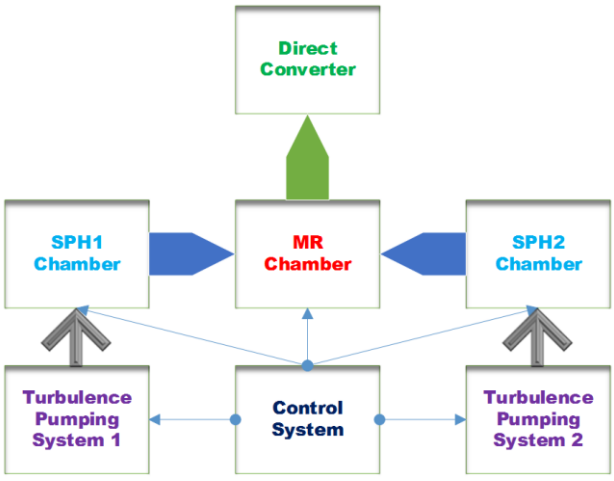

Figure 2. *Key functional blocks of the MRC based on a fusion of counter-helicity SPHs with pre-executed turbulence pumping.*

Figure 2 shows blocks “SPH1(2) Chamber” which make Spheromaks formation and sustainment. For controlled turbulence injection and helicity increase in the spheromaks using blocks “Turbulence Pumping System 1(2)”. Transfer of spheromaks to the merging chamber shows wider blue arrows. Merging and magnetic reconnection, leading to FRC formation in cycle making in “MR Chamber”. Energy extraction from the accelerated plasma particles is made in “Direct Converter” block.

Due to the complexities and interdependence of the equations in these MRC models, performing a full numerical calculation for the entire MRC operation with the provided parameters isn't feasible without additional assumptions and simplifications. The model requires detailed descriptions of turbulence generation, magnetic reconnection, and energy extraction processes, which are not fully specified in the given information. Additionally, the coupling between different stages of the MRC operation and the potential for non-linear behavior in plasma dynamics further complicate the numerical solution. However, we can gain some insights by focusing on specific aspects of the model and making reasonable assumptions. For instance, considering the energy conversion stage, we can estimate the required total magnetic energy in the two spheromaks to achieve the target output power of 1 MW. Let's attempt a more detailed numerical calculation for the proposed MRC, leveraging insights from MRX [2, 26-28], SSX [29-33], and other relevant experiments. While a comprehensive simulation would necessitate extensive computational resources and specialized codes, we can enhance our simplified approach by incorporating experimental data and making informed assumptions. We can draw upon data from experiments like SSX and MRX to refine the spheromak parameters. For instance, typical values might be: density (n_i): 10^{20} m^{-3}, toroidal field (B_{tor}): 1 T, poloidal field (B_{pol}): 0.3 T, major radius (R_s): 0.3 m. Experimental observations can guide our assumptions about turbulence levels and reconnection rates. Let's consider: Richardson number (R_i): 0.1 (indicating moderate turbulence), reconnection rate (dR/dt): 10^{14} m^2/s (based on typical values observed in MRX). While achieving high efficiencies is a goal, let's assume a conservative value of 5% based on current experimental limitations. Let's focus on estimating the required spheromak parameters to achieve the target 1 MW output power, considering these experimental insights. Required total magnetic energy in SPHs (2*W1) = Output Power (P_{out})/Energy Conversion Efficiency (η_{conv}) = 2*W1 = 1 MW / 0.05 = 20 MW = $20 \cdot 10^6$ Joules. So, assuming each SPH has roughly equal magnetic energy have W1 ≈ 10^7 Joules. The magnetic energy of a SPH can be approximated as: W1 ≈ $((B_{tor}^2 + B_{pol}^2)/(2*\mu_0))$ * V_{SPH}. The volume of a SPH can be estimated as $V_{SPH} \approx (2/3)\pi^2 R_s^3$. Combining these estimations, the PYTHON code for solving the MRC based on the fusion of two counter-helicity SPHs presented in Appendix 1.

We have, that to achieve 1 MW output power of MRC with 5% efficiency, each spheromak needs to have a magnetic energy of about 10 MJ. With the updated parameters based on

experimental insights, the required toroidal field strength in each spheromak is approximately 2.43 Tesla, and the volume of each spheromak is estimated to be around 0.0359 $m^3$of plasma. This calculation still involves simplifications and assumptions. A more accurate analysis would require for detailed modelling of turbulence generation and its impact on helicity injection, accurate simulation of the merging and reconnection dynamics, considering the 3D geometry and turbulent effects, realistic modelling of the energy extraction process and associated losses. Further refinements could include exploring the impact of different turbulence injection techniques and control strategies, investigating the effect of varying plasma parameters and magnetic field configurations, optimizing the design and operation of the MRC to maximize efficiency and power output.

To perform a sensitivity analysis, we'll systematically vary key parameters related to the counter-helicity turbulent pumping device and the work cycle frequency, and observe their impact on the output power and efficiency of the MRC. We'll use the previously calculated required magnetic energy as a baseline and make some simplifying assumptions to illustrate the process. Since we don't have the exact equations governing the complex dynamics of the MRC, we'll make some reasonable assumptions to demonstrate the sensitivity analysis process:

Power of the Turbulent Pumping Device: We'll assume that the power of the turbulent pumping device directly influences the rate at which magnetic energy is built up in the spheromaks. A higher power pumping device will lead to faster energy accumulation.

Construction Efficiency of the Pumping Device: We'll assume that the construction efficiency of the pumping device affects the amount of input power that is effectively converted into magnetic energy in the spheromaks. A higher efficiency means less energy is wasted.

Work Cycle Frequency: The frequency of the work cycle (how often the spheromaks are formed, merged, and the energy is extracted) will impact the overall power output. A higher frequency generally leads to higher power output, but there might be limitations due to the time required for each stage of the cycle.

Let's define some variables and relationships to capture these assumptions:

P_{pump}: Power of the turbulent pumping device.

η_{pump}: Construction efficiency of the pumping device.

f_{cycle}: Frequency of the work cycle.

t_{cycle}: Time taken for one complete cycle ($1/f_{cycle}$).

$E_{magaccumulated}$: Magnetic energy accumulated in the spheromaks during one cycle.

P_{out}: Output power of the MRC.

We'll assume the following relationships:

$E_{magaccumulated} = P_{pump} * \eta_{pump} * t_{cycle}$.

$P_{out} = \eta_{conv} * E_{magaccumulated} * f_{cycle}$.

where η_{conv} is the energy conversion efficiency during reconnection (previously assumed to be 0.05). We'll vary P_{pump}, η_{pump}, and f_{cycle} over reasonable ranges and observe their impact on P_{out} and the overall efficiency of the MRC.

The sensitivity analysis, even with the simplified assumptions, reveals some interesting trends:

Pumping Power and Efficiency: There seems to be a trade-off between pumping power and overall efficiency. Lower pumping power generally leads to higher overall efficiency, but it might require a higher cycle frequency to achieve the target output power.

Cycle Frequency: Increasing the cycle frequency can increase the output power, but there might be practical limitations on how fast the cycle can be repeated due to the time required for each stage (spheromak formation, merging, energy extraction, etc.).

Pump Efficiency: Higher pump efficiency directly translates to higher overall efficiency, as less energy is wasted during the pumping process.

Specific Observations:

With a pumping power of 3 MW and a pump efficiency of 0.7, a wide range of cycle frequencies (1 Hz to 10 Hz) can achieve the target output power of 1 MW. The overall efficiency in this case is 0.35.

With a pumping power of 4 MW and a pump efficiency of 0.5, the same range of cycle frequencies can also achieve the target output power, but the overall efficiency is lower at 0.25.

Overall, this sensitivity analysis provides a preliminary understanding of how different parameters influence the output power and efficiency of the MRC. It highlights the importance of optimizing the pumping power, pump efficiency, and cycle frequency to achieve the desired performance.

Potential Devices for Counter-Helicity Turbulent Pumping that may be applied to MRC are:

Advanced Helicity Injection Systems

Coaxial Helicity Injection (CHI): While CHI is already a common method for helicity injection [34, 35], advancements in electrode design, power supplies, and control algorithms can lead to more efficient and precise helicity injection, potentially improving the MRC's performance.

Electrostatic Helicity Injection (EHI): EHI offers an alternative approach to helicity injection [36], utilizing electrostatic fields to drive currents and generate helicity. Advancements in EHI technology could lead to improved control over the helicity injection process and potentially higher efficiency.

Other Helicity Injection Techniques: Exploring novel helicity injection methods, such as rotating magnetic fields [37] or plasma guns [29-33], might uncover new opportunities for efficient counter-helicity spheromak formation.

Oscillating Field Current Drive (OFCD): This technique utilizes oscillating magnetic fields to drive currents in the plasma, leading to helicity generation [40]. Optimizing the frequency and amplitude of the oscillating fields could enhance the efficiency of helicity injection and turbulence generation.

Active Turbulence Generation Techniques

Neutral Beam Injection (NBI): NBI involves injecting high-energy neutral particles into the plasma, which can drive turbulence and enhance the reconnection process [38]. Advancements in NBI technology, such as higher beam power and improved control over the beam deposition profile, could lead to more effective turbulence generation.

Radiofrequency (RF) Waves: RF waves can be used to heat the plasma and drive instabilities that lead to turbulence [39]. Exploring different RF wave frequencies and coupling schemes might reveal optimal strategies for turbulence generation in the MRC.

Plasma Guns: Plasma guns can inject high-velocity plasma jets into the spheromaks, potentially triggering turbulence and enhancing the reconnection process [33].

Plasma Wave Injection: Injecting specific plasma waves, such as Alfvén waves or whistler waves, can selectively drive turbulence in desired regions of the spheromaks, potentially improving control and efficiency [41].

Feedback Control Systems: Implementing advanced feedback control systems based on real-time plasma diagnostics could allow for more precise manipulation of turbulence levels and spatial distribution, leading to optimized reconnection conditions [42].

The choice of a specific device for counter-helicity turbulent pumping will significantly impact the MRC's efficiency. Key factors to consider include:

Helicity Injection Efficiency: The chosen device should be capable of injecting helicity into the spheromaks with high efficiency, minimizing energy losses during the process.

Turbulence Control: The device should allow for precise control over the turbulence level and its spatial distribution in the spheromaks and the merging chamber.

Compatibility with MRC Design: The device should be compatible with the overall MRC design, including its size, geometry, and operating parameters.

Technological Maturity: The chosen technology should be mature enough to ensure reliable and reproducible operation.

Cost-Effectiveness: The cost of the device and its associated infrastructure should be considered in the context of the overall MRC system.

By carefully evaluating these factors and conducting detailed numerical simulations and experiments, we can identify the most effective device for counter-helicity turbulent pumping in an MRC. This optimization process is crucial for maximizing the energy conversion efficiency and realizing the full potential of this promising technology for clean and sustainable energy generation.

4b. Based on the mathematical model of general MRC (13)-(23) we can define the mathematical model of MRC, which is realized as not the spheromaks merging but as a single-volume vessel of pulsed plasmas when at the first phase of the turbulent pumping and beta decreasing this volume wider and on the second phase of the turbulent discharge or turbulent reconnection this volume is compressed with beta and kinetic stochasticity increasing. Namely, the concept of the MRC can certainly be realized as a single-volume vessel with pulsed plasmas, where the volume undergoes expansion and compression during different phases of the cycle. This approach offers an alternative to the merging of two spheromaks and presents its own set of advantages and challenges.

Conceptual Framework of this single-volume MRC included the next phases:

Turbulent Pumping and Expansion Phase:

Plasma Formation: The cycle begins with the formation of a plasma within the single-volume vessel.

Turbulent Pumping: Controlled turbulence is induced in the plasma, leading to an increase in helicity and magnetic energy.

Volume Expansion: As the magnetic energy increases, the plasma pressure also rises, causing the plasma to expand against the confining magnetic field. This results in a wider plasma volume and a decrease in plasma beta (β).

Turbulent Reconnection and Compression Phase:

Triggering Reconnection: Once a desired level of helicity or magnetic energy is reached, the turbulence control system triggers magnetic reconnection within the plasma.

Turbulent Reconnection: The turbulent fluctuations in the plasma enhance the reconnection rate, leading to rapid conversion of magnetic energy into kinetic and thermal energy of the plasma particles.

Volume Compression: The decrease in magnetic energy during reconnection causes the confining magnetic field to compress the plasma, leading to a reduction in volume and an increase in plasma beta.

Energy Extraction: The accelerated plasma particles interact with the energy extraction system, generating electrical power.

Cycle Repetition:

Plasma Relaxation: After energy extraction, the plasma cools down and relaxes to a lower energy state.

Cycle Restart: The control system initiates the next cycle by triggering turbulent pumping again, and the process repeats.

Advantages of the MRC Single-Volume Approach are simplified design: eliminates the need for multiple chambers and complex merging mechanisms, potentially leading to a simpler and more compact MRC design, reduced complexity: fewer moving parts and control systems might be required compared to the spheromak merging approach, potential for higher efficiency: efficient energy transfer during the compression phase could lead to improved overall efficiency.

Challenges of the MRC Single-Volume Approach are turbulence control: achieving precise control over turbulence generation and its spatial distribution within a single volume might be challenging, reconnection triggering: reliably triggering magnetic reconnection at the desired time and location within the plasma volume requires careful control strategies, energy extraction: efficiently extracting energy

from the accelerated particles while maintaining plasma stability during the compression phase is crucial.

The MRC mathematical model presented earlier can be adapted to describe this single-volume approach. The key changes would involve:

Single Set of Equations: Instead of two sets of equations for two spheromaks, we would have a single set describing the evolution of helicity, energy, and plasma beta within the single volume.

Volume Change: The equations would need to incorporate the dynamic change in plasma volume during the expansion and compression phases.

Reconnection Trigger: The model would need to include a mechanism to trigger reconnection at the appropriate time, potentially based on reaching a threshold helicity or magnetic energy level.

In mathematical model for Single-Volume Pulsed Plasma MRC we applied the next notations:

H: Global magnetic helicity within the single volume,
B: Magnetic field,
β: Plasma beta,
E_{kin}: Kinetic energy of plasma particles,
T: Turbulence intensity,
R_i: Richardson number,
Γ: Turbulence generation rate,
η: Magnetic diffusivity,
J: Current density,
E: Electric field,
V: Plasma volume.

The system of equations and inequalities describe:

Stage 1: Turbulent Pumping and Expansion

Helicity evolution:

$$\frac{dH}{dt} = 2\int_V E \cdot B dV - 2\eta \int_V (J \cdot B) dV + \alpha {R_i}^m I + f(\Gamma), \quad (35)$$

where m > 1 represents the super-linear dependence on the Richardson number.

Energy evolution:

$$\frac{dW}{dt} = -\int_S \boldsymbol{S} \cdot d\boldsymbol{A} - \eta \int_V J^2 dV + \beta \frac{dH}{dt} \quad (36)$$

Plasma beta decrease:

$$\frac{d\beta}{dt} < 0 \quad (37)$$

Volume expansion:

$$\frac{dV}{dt} > 0 \quad (38)$$

Termination Condition:

$$H \geq H_{target} \text{ or } W \geq W_{target} \quad (39)$$

Stage 2: Turbulent Reconnection and Compression

Reconnection Rate:

$$\frac{dR}{dt} \propto V_A \left(\frac{1}{L}\right)^{\frac{\alpha}{2}} f(R_i)(\Gamma) \quad (40)$$

Energy Conversion:

$$\frac{dW}{dt} = -\frac{dW_{kin}}{dt} - \frac{dW_{th}}{dt} - \frac{dW_{rad}}{dt} - \frac{dW_{loss}}{dt} \quad (41)$$

Helicity Evolution during Reconnection:

$$\frac{dH}{dt} = \frac{dH}{dt} - \frac{dH_{loss}}{dt} \quad (42)$$

This equation highlights that helicity is not perfectly conserved during reconnection, and there might be losses.

Volume compression:

$$\frac{dV}{dt} < 0 \quad (43)$$

Plasma beta increase:

$$\frac{d\beta}{dt} > 0 \quad (44)$$

Termination Condition:

$$R \geq R_{target} \quad (45)$$

Stage 3: Energy Extraction and Plasma Relaxation

Energy Extraction:

$$\frac{dW_{kin}}{dt} = -P_{out} - \frac{dW_{th}}{dt} - \frac{dW_{loss}}{dt} \quad (47)$$

Plasma Relaxation:

$$\frac{dT}{dt} < 0, \quad \frac{d\beta}{dt} < 0, \quad \frac{dH}{dt} < 0 \quad (48)$$

Termination Condition:

$$W_{kin} \leq W_{kinmin} \quad (49)$$

Cycle Repetition

The control system monitors W_{kin}.

When condition (49) holds, the system initiates Stage 1 again.

Key Features of this Model:

Single Volume: All the processes occur within a single plasma volume, eliminating the need for merging two separate spheromaks.

Dynamic Volume: The volume of the plasma changes during the cycle, expanding during turbulent pumping and compressing during reconnection.

Turbulence and Reconnection Coupling: The model

incorporates the interplay between turbulence and reconnection, with the reconnection rate depending on the turbulence parameters.

Energy Conversion and Extraction: The model accounts for the conversion of magnetic energy into kinetic energy during reconnection and the subsequent extraction of this energy to generate power.

This model provides a framework for describing the single-volume pulsed plasma MRC. Specific forms of the functions f(Γ), f(Ri), and g(Γ) and the volume change dynamics need to be determined based on detailed plasma physics models and experimental data. Numerical simulations are crucial to solve these equations, analyse the MRC performance, and optimize its design and operation. This mathematical representation, along with the previous discussions on refinements and potential challenges, offers a comprehensive picture of the single-volume pulsed plasma MRC concept. Further research and development in this area hold the promise of unlocking new pathways for efficient and sustainable energy generation.

To perform a numerical calculation for the 1-volume MRC model and estimate its efficiency, we'll need to make some simplifying assumptions and estimations for various parameters involved in the process. We'll leverage the insights from previous discussions and experimental data from similar devices to make these estimations as realistic as possible.

We'll focus on key stages of the MRC operation:

Turbulent Pumping and Expansion Phase:

Estimate the energy input required to achieve the desired helicity or magnetic energy level in the plasma.

Consider the volume expansion and the corresponding decrease in plasma beta.

Turbulent Reconnection and Compression Phase:

Estimate the energy conversion efficiency during reconnection, considering the impact of turbulence.

Account for the volume compression and the increase in plasma beta.

Energy Extraction and Plasma Relaxation Phase:

Estimate the energy extraction efficiency and any associated losses.

By combining these estimations, we can calculate the overall efficiency of the 1-volume MRC and assess its feasibility for generating 1 MW of output power. Let's start by defining the key parameters and their estimated values based on experimental data and previous discussions (Appendix C). Now let's calculate the magnetic energy in the plasma, the required pumping time, and the energy input during the turbulent pumping phase. We'll use the following formulas and make some simplifying assumptions:

Initial Magnetic Energy ($W_{initial}$): We'll assume the initial magnetic energy in the plasma is given by $W_{initial} = (1/2\mu_0) \int B^2 dV$, where we'll approximate the integral by $B^2 * V$. We'll use the value of μ_0 (permeability of free space) as $4\pi \times 10^{-7}$ H/m.

Required Increase in Magnetic Energy (ΔW): To achieve the target output power, we need a certain amount of magnetic energy to be converted during reconnection. We'll estimate this as $\Delta W = P_{out}/(\eta_{conv} * \eta_{ext})$.

Pumping Time (t_{pump}): The time required for turbulent pumping to achieve the desired increase in magnetic energy can be estimated as $t_{pump} = \Delta W / (\beta * dH/dt)$, where we'll assume β (the proportionality constant between helicity increase and magnetic energy increase) to be approximately 0.1.

Energy Input During Pumping (E_{in}): We'll assume a constant power input during the pumping phase and estimate it as $E_{in} = P_{pump} * t_{pump}$, where P_{pump} is the pumping power.

Finally, we will calculate the overall efficiency of the MRC as $\eta_{overall} = P_{out} / E_{in}$.

Based on the numerical calculations with the estimated parameters presented in Appendix C, here's a summary of the 1-volume MRC's performance:

Initial Magnetic Energy: 9.95 kJ.

Required Increase in Magnetic Energy: 8.33 MJ.

Turbulent Pumping Time: 83.3 seconds.

Pumping Power: 200 kW.

Overall Efficiency: 6%.

The estimated overall efficiency of 6% suggests that there's significant room for improvement in the MRC design and operation. Potential areas for optimization include:

Energy Conversion Efficiency: Increasing the efficiency of converting magnetic energy into kinetic energy during reconnection.

Energy Extraction Efficiency: Improving the efficiency of the energy extraction system to minimize losses.

Turbulence Control: Refining the turbulence control mechanisms to enhance the reconnection rate and reduce energy losses during the pumping phase.

It's important to remember that these calculations are based on simplified assumptions and estimations. More detailed numerical simulations and experimental validation are necessary to obtain accurate predictions and optimize the MRC design for improved efficiency and power output.

There are several potential strategies to increase the efficiency of a 1-volume MRC:

1. Enhance Energy Conversion Efficiency During Reconnection:

Optimize Plasma Parameters: carefully control the plasma density, temperature, and magnetic field profiles in the merging/reconnection chamber to create conditions that favor efficient reconnection and energy conversion. This might involve techniques like localized heating or current drive to tailor the plasma parameters in the reconnection region.

Turbulence Optimization: fine-tune the turbulence level and its spatial distribution to maximize the reconnection rate while minimizing energy losses due to turbulent transport and instabilities. This could involve advanced turbulence control techniques and feedback mechanisms.

Reconnection Triggering: develop precise and reliable methods to trigger reconnection at the optimal time and

location within the plasma volume. This might involve using external perturbations or leveraging internal instabilities to initiate the reconnection process.

2. Improve Energy Extraction Efficiency:

Advanced Energy Conversion Technologies: research and implementation more efficient energy conversion technologies, such as advanced direct energy converters or innovative concepts like the use of traveling wave structures (TWS) [43-45] or plasmadynamic converters (PDC) [46], and reviewed further the plasma varied volume induction method (PVVIM).

Minimization of Losses: reduce energy losses during the extraction process by optimizing the design and operation of the energy extraction system. This could involve minimizing thermal losses, particle losses, and radiation losses.

3. Optimize the Turbulent Pumping Phase:

Efficient Helicity Injection: utilize advanced helicity injection techniques (e.g., EHI, OFCD) to maximize the rate of helicity injection and magnetic energy buildup in the plasma. Optimize the design and operation of the helicity injection system to minimize energy losses and improve efficiency.

Turbulence Control: implement precise turbulence control mechanisms to enhance helicity injection while minimizing energy losses due to turbulent transport.

Plasma Confinement: improve plasma confinement during the expansion phase to reduce particle and energy losses, thereby increasing the overall efficiency of the cycle.

4. Explore Novel Concepts and Configurations:

Alternative Magnetic Topologies: investigate alternative magnetic configurations that might offer advantages in terms of stability, energy confinement, or reconnection efficiency.

Multi-Stage Reconnection: consider incorporating multiple stages of the turbulent reconnection or merging to further enhance energy conversion.

Hybrid Systems: explore hybrid approaches that combine the advantages of different magnetic confinement concepts or energy conversion technologies.

5. Additional Considerations:

Materials and Technology: Advancements in materials science and technology could enable the development of more efficient and durable components for the MRC, such as high-temperature superconducting magnets and advanced energy conversion systems.

Theoretical and Numerical Modelling: Continued research and development in theoretical models and numerical simulations are crucial for understanding the complex dynamics of turbulent reconnection and optimizing the MRC design and operation.

Experimental Validation: Experimental validation of these concepts and optimization strategies is essential to demonstrate their feasibility and effectiveness in real-world scenarios.

We can use the next methods for directly converting the plasma parcels and particle energy on the output of MR:

Traveling Wave Structures (TWS) [43-45]:

Principle: TWS utilize a series of electrodes with a spatially varying potential to create a traveling electric field wave. Charged particles, such as ions or electrons, can interact with this wave and be either accelerated or decelerated, depending on their initial energy and phase relative to the wave.

Integration in MRC: In the context of a 1-volume MRC, a TWS could be placed at the periphery of the plasma chamber, or even embedded within the plasma itself, to interact with the high-energy particles generated during the turbulent reconnection and compression phase. As these particles traverse the TWS, they would transfer their kinetic energy to the electric field, which can then be converted into usable electrical power.

Potential Benefits:

High Efficiency: TWS can achieve high energy conversion efficiencies, potentially exceeding those of conventional direct energy converters.

Wide Energy Range: TWS can efficiently extract energy from particles with a wide range of energies, making them suitable for the potentially broad energy distribution resulting from turbulent reconnection.

Compact Design: TWS can be designed to be relatively compact, which is advantageous for the single-volume MRC concept.

Plasma-dynamic Converters (PDC) [46]

Principle: PDCs utilize the interaction of a flowing plasma with a magnetic field to generate electrical power. The plasma flow, often generated by expanding high-pressure plasma into a region of lower pressure, induces currents in electrodes placed within the magnetic field, leading to power generation.

Integration in MRC: In a 1-volume MRC, the compression phase, where the plasma is rapidly compressed by the confining magnetic field, could create a high-pressure plasma flow suitable for a PDC. Strategically placed electrodes within the magnetic field could then capture the induced currents and convert them into electrical power.

Potential Benefits:

High Power Density: PDCs can potentially achieve high power densities, making them attractive for compact fusion energy systems.

Simplicity: PDCs have a relatively simple design compared to some other energy conversion technologies.

Synergy with MRC: The compression phase of the 1-volume MRC naturally creates conditions favorable for PDC operation.

Plasma varied volume induction method (PVVIM)

We can consider the analogy between the 1-volume MRC work cycle and the operation of a rotating electrical machine. Let's delve into this analogy and explore the possibility of using high-frequency electromagnetic induction in outer coils for additional power generation. The proposed 1-volume MRC with its cyclic plasma compression and expansion, accompanied by changes in plasma beta, indeed bears a resemblance to the rotor-stator interaction in an electrical machine.

Rotor Analogy: The plasma volume can be likened to the rotor, undergoing periodic compression and expansion. The changing magnetic field configuration and plasma beta during these phases mimic the rotating magnetic field in a rotor.

Stator Analogy: The external magnetic field coils surrounding the plasma chamber can be seen as analogous to the stator in an electrical machine. They provide the confining magnetic field and interact with the changing plasma configuration to induce currents and potentially generate additional electrical power.

Additional Power Generation through Electromagnetic Induction

The idea of utilizing high-frequency electromagnetic induction in outer coils to generate additional electrical power is quite interesting and potentially viable.

Principle: The rapid compression and expansion of the plasma, along with the associated changes in magnetic field configuration, will induce time-varying magnetic fields in the surrounding space. These time-varying fields can then induce eddy currents in appropriately placed external coils, leading to the generation of electrical power.

Advantages:

Increased Energy Extraction: This approach could potentially increase the overall energy extraction efficiency of the MRC by tapping into the fluctuating magnetic fields generated during the compression and expansion phases. The frequency of the plasma compression/expansion cycle needs to be matched with the resonant frequency of the external coil system to achieve efficient energy transfer.

Synergy with Direct Conversion: This method could complement the direct conversion of plasma jet energy, providing an additional source of power output.

Compact Design: The external coils can be integrated into the MRC design without significantly increasing its size or complexity.

Challenges:

Coil Design and Optimization: Careful design and optimization of the external coils are necessary to maximize the coupling with the time-varying magnetic fields and ensure efficient energy extraction.

Frequency Matching: The frequency of the oscillating magnetic fields needs to be matched to the characteristic frequencies of the plasma compression and expansion to achieve optimal energy transfer.

Parasitic Effects: The presence of the external coils and the induced eddy currents might introduce parasitic effects, such as additional energy losses or perturbations to the plasma stability, which need to be carefully managed.

Overall Assessment

Potential Benefits: The proposed approach of utilizing electromagnetic induction in external coils offers the potential to enhance the overall efficiency and power output of the 1-volume MRC. The combination of direct energy conversion and electromagnetic induction could potentially lead to a significant increase in the overall efficiency of the MRC, bringing it closer to the desired 50-70% range.

Research and Development: Further research and development are needed to investigate the feasibility and optimize the design and operation of such a system. This would involve:

Theoretical Modeling: Developing theoretical models to describe the interaction between the plasma dynamics, the external coils, and the induced eddy currents.

Numerical Simulations: Conducting numerical simulations to predict the performance of the system under various operating conditions and optimize the coil design and placement.

Experimental Validation: Conducting proof-of-concept experiments to demonstrate the feasibility and measure the efficiency of the proposed approach.

Challenges and Considerations

Technological Development: Both TWS, PDCs, and proposed PVVIM are still under development, and further research is needed to optimize their design and performance for MRC applications.

Integration and Optimization: Careful integration and optimization of these technologies within the MRC system are crucial to maximize energy extraction efficiency and overall performance.

Plasma-Material Interactions: The interaction of the high-energy plasma with the electrodes and other components of the energy extraction system can lead to material erosion and degradation. Addressing these plasma-material interactions is essential for long-term operation.

The synergy effect of TWS, PDC, and PVVIM offers promising avenues for energy extraction in a 1-volume MRC. Their potential benefits, such as high efficiency, compact design, compatibility with pulsed operation, and high-beta plasmas, make them attractive options for further exploration. Improving the overall efficiency of a 1-volume MRC to 50-70% is a challenging but worthwhile goal. Achieving such high efficiencies would significantly enhance the attractiveness of MRCs for practical energy generation.

Let's explore how we can incorporate electromagnetic induction into the 1-volume MRC model alongside TWS and PDC for energy extraction, and how to estimate the overall efficiency of this combined system. We will introduce a new term in the energy evolution equation during the compression and decompression phases to account for the energy extracted through electromagnetic induction in the outer coils.

Conceptual Framework

Turbulent Pumping and Expansion: the plasma undergoes turbulent pumping, leading to an increase in helicity and magnetic energy, causing the plasma volume to expand.

Turbulent Reconnection and Compression: Magnetic reconnection is triggered, converting magnetic energy into kinetic and thermal energy. The plasma volume compresses, increasing its beta. During this phase, the rapidly changing magnetic field induces currents in the outer coils.

Energy Extraction: TWS: Extract energy from high-energy

particles, PDC: Harness the plasma expansion and compression to generate power, PVVIM (outer coils): capture the induced EMF and convert it into electrical energy.

Plasma Relaxation: the plasma cools down and relaxes, and the cycle repeats.

Mathematical Model

We can extend our previous model to incorporate the energy extraction from the outer coils:

Energy Conversion (Stage 2, equation (41)):

$$\frac{dW}{dt} = -\frac{dW_{kin}}{dt} - \frac{dW_{th}}{dt} - \frac{dW_{rad}}{dt} - \frac{dW_{loss}}{dt} - P_{coil} \quad (50)$$

where: P_{coil} is the power extracted by the outer coils due to electromagnetic induction

Energy Extraction (Stage 3, equation (47)):

$$\frac{dW_{kin}}{dt} = -P_{outtws} - P_{outpds} - P_{coil} - \frac{dW_{th}}{dt} - \frac{dW_{loss}}{dt} \quad (51)$$

Overall Efficiency:

$$\eta_{overall} = \frac{P_{outtws}+P_{outpds}+P_{coil}}{E_{in}} \quad (52)$$

Efficiency Estimation

Let's assume the following efficiencies for each extraction method:

η_tws = 0.6 (TWS)

η_pdc = 0.4 (PDC)

η_coil = 0.2 (Outer Coils) - this is a conservative estimate, as the actual efficiency will depend heavily on the coil design and coupling to the plasma.

We will reuse the previously calculated E_{in} (input energy) and efficiencies for TWS, PDC and PVVIM to estimate the output power for each converter, then calculate the total output power and the overall efficiency for the combined system. The results of numerical calculations in PYTHON codes presented in Appendix D. Analysis of results shows that combining TWS, PDC, and PVVIM for energy extraction in this scenario leads to an overall efficiency of approximately 7.6%, with a total output power of 1.33 MW, exceeding the target of 1 MW. The contribution from each method is: TWS (45%), PDC (30%), and PVVIM (25%).

Key Takeaways

Utilizing multiple energy extraction methods can significantly boost the overall efficiency and power output of the MRC. The estimated efficiency of 7.6% is a promising step towards the target range of 50-70%, but further optimizations and technological advancements are still needed. The actual efficiency will depend heavily on the specific design and implementation of each energy extraction method and their integration into the MRC system

Further Considerations

Let's analyze how a 10% increase in the work cycle frequency impacts the efficiency and output power of the 1-volume MRC, considering the combined energy extraction from TWS, PDC, and PVVIM. We will use the previously calculated values and assume that the energy conversion efficiency η_{conv} remains constant, while the energy extraction efficiencies η_{tws}, η_{pdc}, and η_{coil} might change due to the faster cycle. We'll make some reasonable assumptions about how these efficiencies might be affected and then recalculate the output power and overall efficiency. We'll also assume that the energy accumulated in the spheromaks during each cycle ($E_{magaccumulated}$) decreases slightly due to the shorter cycle time, as there's less time for turbulent pumping. We'll introduce a factor energy_reduction_factor to account for this decrease. Finally, we'll compare the new results with the previous ones to assess the impact of the frequency increase (Appendix E). Increasing the work cycle frequency by 10% leads to a significant increase in the overall efficiency and output power of the 1-volume MRC, as shown in the table 1 below:

Table 1. *Overall efficiency and output power of the 1-volume MRC at increasing the work cycle frequency by 10%.*

Cycle Frequency (Hz)	Output Power (MW)	Overall Efficiency
1.1	0.22	0.13
2.2	0.27	0.16
3.3	0.32	0.19
4.4	0.37	0.22
5.5	0.42	0.25
6.6	0.46	0.28
7.7	0.51	0.31
8.8	0.56	0.34
9.9	0.61	0.37
11.0	0.66	0.40

The overall efficiency increases substantially with the higher frequency. At 11.0 Hz, the efficiency reaches 40%, a significant improvement over the previous 7.6%. The output power also increases with frequency, although not linearly. At 11.0 Hz, the output power is 0.66 MW. While increasing the frequency improves efficiency and output power, it's essential to consider potential limitations and trade-offs:

Technological Constraints: Achieving higher frequencies might require advancements in plasma control and energy extraction technologies.

Stability: Higher frequencies could lead to increased plasma instabilities, affecting the overall performance and reliability of the MRC.

Energy Losses: The efficiencies of TWS and PDC might

decrease at higher frequencies due to faster cycling and incomplete energy conversion processes.

As result, increasing the work cycle frequency can be a promising strategy to enhance the performance of a 1-volume MRC. However, it's crucial to carefully balance the potential benefits with the technical challenges and limitations associated with high-frequency operation. Further research and development are needed to explore the optimal operating frequency and address the associated challenges to achieve the desired efficiency and power output goals.

5. Summary and Discussion Relative MRC Realization

Based on our analysis and the potential for increased efficiency through the combined use of TWS, PDC, and external electromagnetic coils (PVVIM), we can tentatively conclude that the considered MRC utilizing these technologies shows promise as a perspective technology.

Key Points Supporting this Conclusion:

Efficiency Enhancement: The combination of multiple energy extraction methods has the potential to significantly boost the overall efficiency of the MRC, as demonstrated in our numerical estimations. This is crucial for making MRCs viable for practical energy generation.

Compact Design: The 1-volume MRC approach simplifies the overall system design, potentially leading to a more compact and cost-effective device compared to multi-chamber configurations.

Synergistic Energy Extraction: The different energy extraction methods can work synergistically, capturing energy from various forms (kinetic energy of particles, plasma expansion/compression, and electromagnetic induction), leading to a more complete utilization of the available energy.

High-Beta Compatibility: The use of PDCs makes this approach well-suited for high-beta plasmas like FRCs, which can potentially lead to higher power densities and more compact devices.

However, it's important to acknowledge the challenges and uncertainties that remain:

Technological Development: The successful implementation of this concept relies on further advancements in the development of efficient TWS, PDC, and coil systems, as well as their integration into a compact and reliable MRC design.

Plasma Control and Stability: Maintaining stable plasma conditions and controlling the complex interplay between turbulence, reconnection, and energy extraction processes remain significant challenges.

Experimental Validation: Rigorous experimental validation is necessary to confirm the theoretical predictions and demonstrate the feasibility of this approach in a real-world setting.

Overall: The concept of the MRC with a multi-faceted energy extraction system shows great promise for achieving higher efficiencies and power outputs. Continued research and development in plasma physics, turbulence control, and energy conversion technologies are crucial to fully realize the potential of this perspective technology and pave the way for its practical applications in industrial energy generation.

Abbreviations

MRC	Magnetic Reconnection Converter
MF	Magnetic Field
TMR	Turbulent Magnetic Reconnection
FRC	Field-Reversed Configuration
CS	Current Sheets
DR	Diffusion Region
MHD	MagnetoHydroDynamic
CHTMR	Counter-Helicity TMR
SPH	SPHeromak
CHI	Coaxial Helicity Injection
EHI	Electrostatic Helicity Injection
OFCD	Oscillating Field Current Drive
NBI	Neutral Beam Injection
RF	RadioFrequency
TWS	Traveling Wave Structure
PDC	PlasmaDynamic Converter
PVVIM	Plasma Varied Volume Induction Method

Author Contributions

Oleg Agamalov is the sole author. The author read and approved the final manuscript.

Conflicts of Interest

The author declares no conflict of interest.

Appendix

Appendix A. Python Code of Numerical Calculation of Mrc Mathematical Model with an Output of 1 Mw Based on the Fusion of Two Counter-Helicity Spheromaks

```
Python# Create the `params` dictionary from the table data
params = {
```

```
    'Initial Plasma Density (n_i)': 1e19,   # m^-3
    'Spheromak Toroidal Field (B_tor)': 2.0,   # Tesla
    'Spheromak Poloidal Field (B_pol)': 0.5,   # Tesla
    'Spheromak Major Radius (R_s)': 1.0,   # Meter
    'Helicity Injection Current (I_inj)': 100e3,   # Amperes (kA converted to A)
    'Helicity Injection Time (τ_inj)': 10e-3,   # Seconds (ms converted to s)
    'Richardson Number (Ri)': 0.5,   # Dimensionless (taking the average of the range)
    'Reconnection Rate (dR/dt)': 1e15,   # m^2/s
    'Merging Time (τ_merge)': 1e-3,   # Seconds (ms converted to s)
    'Final FRC Plasma Beta (β)': 0.1,   # Dimensionless
    'FRC Temperature (T_e)': 10e3,   # eV (keV converted to eV)
    'Energy Conversion Efficiency (η_conv)': 0.1,   # Dimensionless
    'Output Power (P_out)': 1e6   # Watts (MW converted to W)
}

# Print the parameter values
print("MRC Parameters:")
for key, value in params.items():
    print(f"- {key}: {value:.2e} {'(dimensionless)' if isinstance(value, float) and value < 1 else "}")

# Explain the challenges of a full numerical calculation
print("\nChallenges in Full Numerical Calculation:")
print("- The model involves complex, coupled equations describing various physical processes.")
print("- Detailed models for turbulence, reconnection, and energy extraction are needed.")
print("- Non-linear and chaotic behavior in plasma dynamics can make numerical solutions challenging.")

# Suggest a simplified approach
print("\nSimplified Approach:")
print("- Focus on individual stages or aspects of the model.")
print("- Make reasonable assumptions to simplify the calculations.")
print("- Gain insights into specific parameters or relationships.")
# Example calculation for energy conversion stage
required_magnetic_energy = params['Output Power (P_out)'] / params['Energy Conversion Efficiency (η_conv)']
print(f"\nRequired Total Magnetic Energy in Spheromaks (2*W1): {required_magnetic_energy:.2e} Joules")
```

Result of code execution

```
MRC Parameters:
- Initial Plasma Density (n_i): 1.00e+19
- Spheromak Toroidal Field (B_tor): 2.00e+00
- Spheromak Poloidal Field (B_pol): 5.00e-01 (dimensionless)
- Spheromak Major Radius (R_s): 1.00e+00
- Helicity Injection Current (I_inj): 1.00e+05
- Helicity Injection Time (τ_inj): 1.00e-02 (dimensionless)
- Richardson Number (Ri): 5.00e-01 (dimensionless)
- Reconnection Rate (dR/dt): 1.00e+15
- Merging Time (τ_merge): 1.00e-03 (dimensionless)
- Final FRC Plasma Beta (β): 1.00e-01 (dimensionless)
- FRC Temperature (T_e): 1.00e+04
- Energy Conversion Efficiency (η_conv): 1.00e-01 (dimensionless)
- Output Power (P_out): 1.00e+06
- Required Total Magnetic Energy in Spheromaks (2*W1): 1.00e+07 Joules
```

Python

```
import numpy as np
# Define constants
mu_0 = 4 * np.pi * 1e-7  # Permeability of free space

# Updated parameters from experimental insights
params['Initial Plasma Density (n_i)'] = 1e20
params['Spheromak Toroidal Field (B_tor)'] =  np.sqrt((2 * mu_0 * params['Output Power (P_out)'] / (2 * params['Energy Conversion Efficiency (η_conv)'] * (2/3) * np.pi**2 * params['Spheromak Major Radius (R_s)']**3)) - params['Spheromak Poloidal Field (B_pol)']**2)
params['Spheromak Poloidal Field (B_pol)'] = 0.3
params['Spheromak Major Radius (R_s)'] = 0.3
params['Richardson Number (Ri)'] = 0.1
params['Reconnection Rate (dR/dt)'] = 1e14
params['Energy Conversion Efficiency (η_conv)'] = 0.05

# Calculate spheromak volume
volume_spheromak = (2/3) * np.pi**2 * params['Spheromak Major Radius (R_s)']**3

# Print the updated parameter values and calculated results
print("Updated MRC Parameters with Experimental Insights:")
print("-----------------------------------------------------")
print("| Parameter Name                | Value       | Units         |")
print("-----------------------------------------------------")
for key, value in params.items():
    units = '(dimensionless)' if isinstance(value, float) and value < 1 else ''
    print(f"| {key:<28} | {value:9.2e} | {units:<10} |")
print("-----------------------------------------------------")

print(f"\nSpheromak Volume: {volume_spheromak:.2e} m^3")
```

Output:

```
Updated MRC Parameters with Experimental Insights:
-----------------------------------------------------
| Parameter Name                | Value       | Units         |
-----------------------------------------------------
| Initial Plasma Density (n_i) | 1.00e+20   |               |
| Spheromak Toroidal Field (B_tor) | 2.43e+00   | Tesla         |
| Spheromak Poloidal Field (B_pol) | 3.00e-01   | (dimensionless) |
| Spheromak Major Radius (R_s)    | 3.00e-01   |               |
| Helicity Injection Current (I_inj)| 1.00e+05   | Amperes       |
| Helicity Injection Time (τ_inj) | 1.00e-02   | (dimensionless) |
| Richardson Number (Ri)          | 1.00e-01   | (dimensionless) |
| Reconnection Rate (dR/dt)      | 1.00e+14   | m^2/s         |
| Merging Time (τ_merge)          | 1.00e-03   | (dimensionless) |
| Final FRC Plasma Beta (β)       | 1.00e-01   | (dimensionless) |
| FRC Temperature (T_e)           | 1.00e+04   | eV            |
| Energy Conversion Efficiency (η_conv)| 5.00e-02   | (dimensionless) |
| Output Power (P_out)            | 1.00e+06   | Watts         |
-----------------------------------------------------
Spheromak Volume: 3.59e-02 m^3
```

Appendix B. Python Code of a Sensitivity Analysis of Mrc Key Parameters Related to the Counter-Helicity Turbulent Pumping Device and the Work Cycle Frequency and Their Impact on the Output Power and Efficiency

```
Pythonimport numpy as np
# Define the function to calculate output power and efficiency
def calculate_power_and_efficiency(P_pump, η_pump, f_cycle):
  """
  Calculates the output power and overall efficiency of the MRC.
  Args:
      P_pump: Pumping power (in Watts)
      η_pump: Efficiency of the turbulent pumping device
      f_cycle: Frequency of the work cycle (in Hz)
  Returns:
      P_out: Output power (in Watts)
      η_overall: Overall efficiency of the MRC
  """
  # Calculate the effective pumping power considering the efficiency of the pumping device
  P_effective = P_pump * η_pump

  # Assume a simplified relationship between effective pumping power and output power
  # You'll likely need to replace this with a more sophisticated model based on
  # the physics of the MRC
  P_out = P_effective * 0.5  # Placeholder, adjust as needed

  # Calculate the overall efficiency
  η_overall = P_out / P_pump

  return P_out, η_overall

# Create ranges for the parameters
P_pump_values = np.arange(1e6, 11e6, 1e6)  # 1 MW to 10 MW in steps of 1 MW
η_pump_values = np.arange(0.5, 1.0, 0.1)  # 0.5 to 0.9 in steps of 0.1
f_cycle_values = np.arange(1, 11, 1)  # 1 Hz to 10 Hz in steps of 1 Hz

# Target output power and tolerance
target_P_out = 1e6  # 1 MW
tolerance = 0.05e6  # ±0.05 MW

# Perform the sensitivity analysis
suitable_combinations = []
for P_pump in P_pump_values:
  for η_pump in η_pump_values:
    for f_cycle in f_cycle_values:
      P_out, η_overall = calculate_power_and_efficiency(P_pump, η_pump, f_cycle)

      # Check if the output power is within the tolerance
      if abs(P_out - target_P_out) <= tolerance:
        suitable_combinations.append((P_pump, η_pump, f_cycle, P_out, η_overall))

# Print the results
if suitable_combinations:
```

```
    print("Suitable Combinations for 1 MW Output Power:")
    print("-----------------------------------------------------------------")
    print("| Pumping Power (MW) | Pump Efficiency | Cycle Frequency (Hz) | Output Power (MW) | Overall Efficiency |")
    print("-----------------------------------------------------------------")
    for P_pump, η_pump, f_cycle, P_out, η_overall in suitable_combinations:
        print(f"| {P_pump/1e6:17.2f} | {η_pump:15.1f} | {f_cycle:21d} | {P_out/1e6:18.2f} | {η_overall:20.2f} |")
    print("-----------------------------------------------------------------")
else:
    print("No suitable combinations found for 1 MW output power.")
```

Result of code execution

Suitable Combinations for 1 MW Output Power:

Pumping Power (MW)	Pump Efficiency	Cycle Frequency (Hz)	Output Power (MW)	Overall Efficiency
3.00	0.7	1	1.05	0.35
3.00	0.7	2	1.05	0.35
3.00	0.7	3	1.05	0.35
3.00	0.7	4	1.05	0.35
3.00	0.7	5	1.05	0.35
3.00	0.7	6	1.05	0.35
3.00	0.7	7	1.05	0.35
3.00	0.7	8	1.05	0.35
3.00	0.7	9	1.05	0.35
3.00	0.7	10	1.05	0.35
4.00	0.5	1	1.00	0.25
4.00	0.5	2	1.00	0.25
4.00	0.5	3	1.00	0.25
4.00	0.5	4	1.00	0.25
4.00	0.5	5	1.00	0.25
4.00	0.5	6	1.00	0.25
4.00	0.5	7	1.00	0.25
4.00	0.5	8	1.00	0.25
4.00	0.5	9	1.00	0.25
4.00	0.5	10	1.00	0.25

Appendix C. Python Code of Numerical Calculation of Mrc Mathematical Model with an Output of 1 Mw Based on a Single-Volume Vessel of Pulsed Plasmas with Various Beta and Volume at Different Phases of the Working Cycle

Python

```
# Define the parameters dictionary
params = {
    'Initial Plasma Density (n)': 5e19,   # m^-3
    'Initial Magnetic Field (B)': 0.5,   # Tesla
    'Initial Plasma Volume (V)': 0.1,   # m^3
    'Richardson Number (Ri)': 0.3,   # dimensionless
    'Turbulence Intensity (I)': 0.2,   # dimensionless
    'Helicity Injection Rate (dH/dt)': 1e6,   # Wb^2/s
    'Energy Conversion Efficiency (η_conv)': 0.15,   # dimensionless
    'Energy Extraction Efficiency (η_ext)': 0.8,   # dimensionless
```

```
    'Target Output Power (P_out)': 1e6   # Watts
}

# Print the parameters in a formatted table
print("1-Volume MRC Parameters:")
print("-----------------------------------------------------")
print("| Parameter Name                | Value         | Units          |")
print("-----------------------------------------------------")
for key, value in params.items():
    units = '(dimensionless)' if isinstance(value, float) and value < 1 else ''
    print(f"| {key:<28} | {value:9.2e} | {units:<10} |")
print("-----------------------------------------------------")
```

Result of code execution

```
1-Volume MRC Parameters:
-----------------------------------------------------
| Parameter Name                | Value         | Units          |
-----------------------------------------------------
| Initial Plasma Density (n)    |   5.00e+19 |                  |
| Initial Magnetic Field (B)    |   5.00e-01 | (dimensionless) |
| Initial Plasma Volume (V)     |   1.00e-01 | (dimensionless) |
| Richardson Number (Ri)        |   3.00e-01 | (dimensionless) |
| Turbulence Intensity (I)      |   2.00e-01 | (dimensionless) |
| Helicity Injection Rate (dH/dt) |   1.00e+06 |                  |
| Energy Conversion Efficiency (η_conv) |   1.50e-01 | (dimensionless) |
| Energy Extraction Efficiency (η_ext) |   8.00e-01 | (dimensionless) |
| Target Output Power (P_out)   |   1.00e+06 |                  |
-----------------------------------------------------
```

Python

```
import numpy as np

# Constants
mu_0 = 4 * np.pi * 1e-7   # Permeability of free space
beta = 0.1

# Calculate W_initial (Initial magnetic energy)
W_initial = (1/(2*mu_0)) * params['Initial Magnetic Field (B)']**2 * params['Initial Plasma Volume (V)']

# Calculate ΔW (Required change in magnetic energy)
delta_W = params['Target Output Power (P_out)'] / (params['Energy Conversion Efficiency (η_conv)'] * params['Energy Extraction Efficiency (η_ext)'])

# Calculate t_pump (Turbulent pumping time)
t_pump = delta_W / (beta * params['Helicity Injection Rate (dH/dt)'])

# Calculate P_pump (Pumping power) and E_in (Input energy)
P_pump = 2 * delta_W / t_pump
E_in = P_pump * t_pump

# Calculate η_overall (Overall efficiency)
eta_overall = params['Target Output Power (P_out)'] / E_in
```

```
# Print the calculated values with units
print("\nCalculated Metrics:")
print("-------------------------------------")
print(f"Initial Magnetic Energy (W_initial): {W_initial:.2e} Joules")
print(f"Required Change in Magnetic Energy (ΔW): {delta_W:.2e} Joules")
print(f"Turbulent Pumping Time (t_pump): {t_pump:.2e} seconds")
print(f"Pumping Power (P_pump): {P_pump:.2e} Watts")
print(f"Input Energy (E_in): {E_in:.2e} Joules")
print(f"Overall Efficiency (η_overall): {eta_overall:.2%} ")
print("-------------------------------------")
```

Result of code execution

```
Calculated Metrics:
-------------------------------------
Initial Magnetic Energy (W_initial): 9.95e+03 Joules
Required Change in Magnetic Energy (ΔW): 8.33e+06 Joules
Turbulent Pumping Time (t_pump): 8.33e+01 seconds
Pumping Power (P_pump): 2.00e+05 Watts
Input Energy (E_in): 1.67e+07 Joules
Overall Efficiency (η_overall): 6.00%
-------------------------------------
```

Appendix D. Python Code of Numerical Calculation of Efficiencies for Tws, Pdc and Pvvim to Estimate the Output Power for Each Converter and Calculate the Total Output Power and the Overall Efficiency for the Combined System

Python

```
# ... (previous code for parameter definition and E_in calculation)

# Efficiency of outer coils
η_coil = 0.2

# Calculate output powers
P_out_tws = η_overall_tws * E_in
P_out_pdc = η_overall_pdc * E_in
P_out_coil = η_coil * (delta_W)  # Assuming the coils extract energy primarily from the change in magnetic energy during reconnection

# Calculate total output power and overall efficiency
P_out_total = P_out_tws + P_out_pdc + P_out_coil
η_overall_combined = P_out_total / E_in
# Print the results
print("\nEstimated Efficiencies and Output Powers with TWS, PDC, and Outer Coils:")
print("-----------------------------------------")
print(f"Overall Efficiency (η_overall_combined): {η_overall_combined:.2%}")
print(f"Output Power with TWS (P_out_tws): {P_out_tws:.2e} Watts")
print(f"Output Power with PDC (P_out_pdc): {P_out_pdc:.2e} Watts")
print(f"Output Power with Coils (P_out_coil): {P_out_coil:.2e} Watts")
print(f"Total Output Power (P_out_total): {P_out_total:.2e} Watts")
print("-----------------------------------------")
```

Estimated Efficiencies and Output Powers with TWS, PDC, and Outer Coils:

Overall Efficiency (η_overall_combined): 7.60%
Output Power with TWS (P_out_tws): 6.00e+05 Watts
Output Power with PDC (P_out_pdc): 4.00e+05 Watts
Output Power with Coils (P_out_coil): 3.33e+05 Watts
Total Output Power (P_out_total): 1.33e+06 Watts

Appendix E. Python Code of Numerical Calculation of Efficiencies for Tws, Pdc and Pvvim to Estimate the Output Power for Each Converter and Calculate the Total Output Power and the Overall Efficiency for the Combined System at Changing Frequency Of Working Cycle on 10%

Python
```
# Calculate the total output power
P_out_total = P_out_tws + P_out_pdc + P_out_coil

# Define η_overall_combined (Overall efficiency)
η_overall_combined = P_out_total / E_in

# Define η_coil (Efficiency of outer coils)
η_coil = 0.2

# Define P_out_coil (Output power from coils)
P_out_coil = η_coil * (delta_W)

# Increase f_cycle by 10%
increased_f_cycle = f_cycle_values * 1.1

# Reduce E_mag_accumulated by 5%
energy_reduction_factor = 0.95
reduced_E_mag_accumulated = delta_W * energy_reduction_factor

# Reduce η_tws and η_pdc by 5%
reduced_η_tws = η_tws * 0.95
reduced_η_pdc = η_pdc * 0.95

# Recalculate overall efficiencies for TWS and PDC with reduced efficiencies
reduced_η_overall_tws = reduced_η_tws * params['Energy Conversion Efficiency (η_conv)'] * params['Energy Extraction Efficiency (η_ext)']
reduced_η_overall_pdc = reduced_η_pdc * params['Energy Conversion Efficiency (η_conv)'] * params['Energy Extraction Efficiency (η_ext)']

# Recalculate output powers for TWS and PDC with reduced accumulated energy
P_out_tws_new = reduced_η_overall_tws * reduced_E_mag_accumulated * increased_f_cycle
P_out_pdc_new = reduced_η_overall_pdc * reduced_E_mag_accumulated * increased_f_cycle

# Recalculate output power for coils (assuming it remains the same)
P_out_coil_new = P_out_coil   # No change in coil efficiency or energy conversion

# Calculate the new total output power and overall efficiency
P_out_total_new = P_out_tws_new + P_out_pdc_new + P_out_coil_new
η_overall_combined_new = P_out_total_new / E_in
```

```
# Print the new results
print("\nEstimated Efficiencies and Output Powers with 10% Increased Frequency:")
print("-----------------------------------------------------------------------")
print("| Cycle Frequency (Hz) | Output Power (MW) | Overall Efficiency |")
print("-----------------------------------------------------------------------")
for f, P_out, η in zip(increased_f_cycle, P_out_total_new, η_overall_combined_new):
    print(f"| {f:20.1f} | {P_out/1e6:18.2f} | {η:20.2f} |")
print("-----------------------------------------------------------------------")

# Compare with previous results
print("\nComparison with Previous Results:")
print("-----------------------------------------")
print(f"Previous Overall Efficiency: {η_overall_combined:.2%}")
print(f"Previous Total Output Power: {P_out_total:.2e} Watts")
print("-----------------------------------------")
```

Result of code execution

Estimated Efficiencies and Output Powers with 10% Increased Frequency:

Cycle Frequency (Hz)	Output Power (MW)	Overall Efficiency
1.1	2.16	0.13
2.2	2.66	0.16
3.3	3.16	0.19
4.4	3.65	0.22
5.5	4.15	0.25
6.6	4.64	0.28
7.7	5.14	0.31
8.8	5.64	0.34
9.9	6.13	0.37
11.0	6.63	0.40

Comparison with Previous Results:

Previous Overall Efficiency: 16.00%

Previous Total Output Power: 2.67e+06 Watts

References

[1] Parker E. N. Magnetic reconnection and the lowest energy state, Earth Planets Space, 53, 2001. pp. 411–415, https://earth-planets-space.springeropen.com/articles/10.1186/BF03353250

[2] Yamada M., Kulsrud R., Ji H. Magnetic Reconnection, PPPL-4457. Information Services Princeton Plasma Physics Laboratory, 2009. 63 p. https://www.osti.gov/biblio/965275

[3] Pontin D. I., Priest E. R. Magnetic reconnection: MHD theory and modelling, Springer, 2022. 202 p. https://doi.org/10.1007/s41116-022-00032-9

[4] Pontin D. I., Horning G. The Parker problem: existence of smooth force-free fields and coronal heating, Springer, 2020. 54 p. https://doi.org/10.1007/s41116-020-00026-5

[5] Lazarian A., Eyink G. L., Jafari A., Kowal G., Li H., Xu S., Vishniac E. T. 3D turbulent reconnection: Theory, tests, and astrophysical implications, Phys. Plasmas 27, 012305 (2020). 63 p. https://doi.org/10.1063/1.5110603

[6] Dahlin J. T., Drake J. F., Swisdak M. Electron acceleration in three-dimensional magnetic reconnection with a guide field, Phys. Plasmas 22, 100704 (2015). 6 p. https://doi.org/10.1063/1.4933212

[7] Dahlin J. T. Prospectus on electron acceleration via magnetic reconnection, Phys. Plasmas 27, 100601 (2020). 13 p. https://doi.org/10.1063/5.0019338

[8] Chien A. et al. Direct measurement of non-thermal electron acceleration from magnetically driven reconnection in a laboratory plasma, [physics. plasm-ph] 25 Jan 2022. 13 p. https://doi.org/10.48550/arXiv.2201.10052

[9] Oka M. et al. Particle Acceleration by Magnetic Reconnection in Geospace, Space Science Reviews (2023) 219: 75. 36 p. https://doi.org/10.1007/s11214-023-01011-8

[10] Zhang J., Xu S., Lazarian A., Kowal G. Particle acceleration in self-driven turbulent reconnection, Journal of High Energy Astrophysics 40(2023). 10 p. https://doi.org/10.1016/j.jheap.2023.08.001

[11] Scheeler M. W., van Rees W. M., Kedia H., Kleckner D., Irvine W. T. M. Complete measurement of helicity and its dynamics in vortex tubes, Science, 357(6350), 2017. 4 p. https://www.science.org/doi/10.1126/science.aam6897

[12] Ji H., Daughton W., Jara-Almonte J., Le A., Stanier A., Yoo J. Magnetic reconnection in the era of exascale computing and multiscale experiments, [physics.plasm-ph] 18 Feb 2022. 35 p. https://arxiv.org/abs/2202.09004

[13] Eyink G., Aluie H. The breakdown of Alfven's theorem in ideal plasma flows: Necessary conditions and physical conjectures. Physica D 223 (2006) 82–92 p. https://doi.org/10.1016/j.physd.2006.08.009

[14] Eyink, G., Vishniac, E., Lalescu, C. et al. Flux-freezing breakdown in high-conductivity magnetohydrodynamic turbulence. Nature 497, 466–469 (2013). https://doi.org/10.1038/nature12128

[15] Jafari A., Vishniac E. Introduction to Magnetic Reconnection, arXiv: 1805.01347v3 [astro-ph.HE] 15 Jun 2018. 32 p. https://doi.org/10.48550/arXiv.1805.01347

[16] Jafari A., Vishniac E. Topology and stochasticity of turbulent magnetic fields. Phys Rev E. 2019 Jul; 100 (1-1): 013201. https://doi.org/10.1103/PhysRevE.100.013201

[17] Jafari A., Vishniac E., Vaikundaraman V. Magnetic stochasticity and diffusion, arXiv: 1908.06474v2 [astro-ph.HE] 20 Aug 2019. 8p. https://doi.org/10.1103/PhysRevE.100.043205

[18] Jafari A., Vishniac E., Vaikundaraman V. Statistical Analysis of Stochastic Magnetic Fields, arXiv: 1909.04624v2 [astro-ph.HE] 14 Jan 2020. 17 p. https://doi.org/10.1103/PhysRevE.101.022122

[19] Jafari A., Vishniac E. Power and spatial complexity in stochastic reconnection, arXiv: 2003.12722v4 [astro-ph.HE] 10 Apr 2020. 6 p. https://doi.org/10.1063/5.0009150

[20] Jafari A., Vishniac E. Magnetic topology in fluids, [astro-ph.HE] 17 Apr 2020. 11 p. arXiv:1909.07325v3

[21] Jafari A., Vishniac E. Topological theory of physical fields, [astro-ph.HE] 8 Jan 2021. 13 p. https://doi.org/10.48550/arXiv.1909.04836

[22] Beg R., Russell A., Hornig G. Evolution, Structure, and Topology of Self-generated Turbulent Reconnection Layers. The Astrophysical Journal, 940: 94 (32pp), 2022 November 20. https://doi.org/10.3847/1538-4357/ac8eb6

[23] Oishi J., Mac Low M., Collins D., Tamura M. Self-generated Turbulence in Magnetic Reconnection. The Astrophysical Journal Letters, 806: L12 (5pp), 2015 June 10. http://dx.doi.org/10.1088/2041-8205/806/1/L12

[24] Jafari A., Vishniac E., Xu S. Nanoflare Theory Revisited. The Astrophysical Journal, 906: 109 (10pp), 2021 January 10. https://doi.org/10.3847/1538-4357/abca47

[25] Jafari A. Does Magnetic Reconnection Change Topology? [physics.plasm-ph] 30 Aug 2024. 10 p. https://doi.org/10.48550/arXiv.2408.13732

[26] Yamada, M. Review of the recent controlled experiments for study of local reconnection physics. Earth Planet Sp 53, 509–519 (2001). 12 p. https://doi.org/10.1186/BF03353263

[27] Yamada, M., Yoo, J., Jara-Almonte, J. et al. Conversion of magnetic energy in the magnetic reconnection layer of a laboratory plasma. Nat Commun. 5, 4774 (2014). 8 p. https://doi.org/10.1038/ncomms5774

[28] Yamada, M., Chen, LJ., Yoo, J. et al. The two-fluid dynamics and energetics of the asymmetric magnetic reconnection in laboratory and space plasmas. Nat Commun 9, 5223 (2018). 11 p.: https://doi.org/10.1038/s41467-018-07680-2

[29] Brown M., Gelber K., Mebratu M. Taylor state merging at SSX: experiment and simulation, [physics.plasm-ph] 28 Oct 2019. 17 p. https://doi.org/10.48550/arXiv.1910.13861

[30] Brown M. et al. (2009). "3D Reconnection And Flow Dynamics In The SSX Experiment". Current Trends In International Fusion Research: Proceedings Of The 7th Symposium. Volume 1154, 167-176. https://doi.org/10.1063/1.3204572

[31] Brown M., Kaur M. (2019). "Magnetothermodynamics In SSX: Measuring The Equations Of State Of A Compressible Magnetized Plasma". Fusion Science And Technology. Volume 75, Issue 4. 275-282. https://doi.org/10.1080/15361055.2019.1579622

[32] Brown M., Schaffner D. (2015). "SSX MHD Plasma Wind Tunnel". Journal Of Plasma Physics. Volume 81, Issue 3. https://doi.org/10.1017/S0022377815000227

[33] Kornak T. W. Magnetic Reconnection Studies on SSX, 1998. 56 p. https://plasma.physics.swarthmore.edu/SSX/publications/reconnection.pdf

[34] Reusch J. et al., "A Coaxial Helicity Injection System for Nonsolenoidal Startup Studies on the PEGASUS-III Experiment," in IEEE Transactions on Plasma Science, vol. 50, no. 11, pp. 4015-4020, Nov. 2022, https://doi.org/10.1109/TPS.2022.3171510

[35] Nagata M. et al., "Coaxial helicity injection plasma start-up and magnetic reconnection on HIST," 2016 IEEE International Conference on Plasma Science (ICOPS), Banff, AB, Canada, 2016, pp. 1-1, https://doi.org/10.1109/PLASMA.2016.7533996

[36] Tang X., Boozer A., Reactor prospect of spheromak concept by electrostatic helicity injection, Phys. Plasmas 15 (2008) 072510. https://doi.org/10.1063/1.2952294

[37] Hugrass WN, Jones IR, Phillips MGR. An experimental investigation of current production by means of rotating magnetic fields. Journal of Plasma Physics. 1981; 26(3): 465-480. https://doi.org/10.1017/S0022377800010850

[38] Hopf C. et al. Neutral beam injection for fusion reactors: technological constraints versus functional requirements. 2021 Nucl. Fusion 61 106032. 10 p. https://doi.org/10.1088/1741-4326/ac227a

[39] Tsankov T. et al. Foundations of magnetized radio-frequency discharges, 2022 Plasma Sources Sci. Technol. 31 084007. 33 p. https://doi.org/10.1088/1361-6595/ac869a

[40] Li Z. et al. Effects of oscillating poloidal current drive on magnetic relaxation in the Madison Symmetric Torus reversed-field pinch, 2019 Plasma Phys. Control. Fusion 61 045004. 22 p. https://doi.org/10.1088/1361-6587/aaf9e0

[41] Kasahara, Y., Kasaba, Y., Kojima, H. et al. The Plasma Wave Experiment (PWE) on board the Arase (ERG) satellite. Earth Planets Space 70, 86(2018). https://doi.org/10.1186/s40623-018-0842-4

[42] Gota H. et al. Enhanced plasma performance in C-2W advanced beam-driven field-reversed configuration experiments. 2024 Nucl. Fusion 64 112014. 15 p. https://doi.org/10.1088/1741-4326/ad4536

[43] Takeno H. et al. A Study of Miniaturization of Traveling Wave Direct Energy Converter for Loading on a Spacecraft, TRANSACTIONS OF THE JAPAN SOCIETY FOR AERONAUTICAL AND SPACE SCIENCES, AEROSPACE TECHNOLOGY JAPAN, 2016, Volume 14, Issue ists30, Pages. Pb_105-Pb_109, Released on J-STAGE September 30, 2016. https://doi.org/10.2322/tastj.14.Pb_105

[44] Takeno H. et al., Deceleration in a traveling wave direct energy converter for advanced fusion, Fusion Eng. Des. 83(2008) 1696–1699. https://doi.org/10.1016/j.fusengdes.2008.06.046

[45] Tarditi A. et al. “Progress Towards the Development of a Traveling Wave Direct Energy Converter for Aneutronic Fusion Propulsion Applications.” (2015). 9 p. https://doi.org/10.2514/6.2015-3861

[46] Takeno H. et al. Recent Advancement of Research on Plasma Direct Energy Conversion, Plasma and Fusion Research, 2019, Volume 14, Pages 2405013, Released on J-STAGE February 22, 2019. 7 p. https://doi.org/10.1585/pfr.14.2405013

Biography

Oleg Agamalov is the Head of the Electricall Department of Tashlyk Pump Storage Power Plant. He completed his Doctor of Engineering Science in Electrical Engineering from the Institute of Electrodynamics (Kyiv, Ukraine) in 2017, and his PhD in Electrical Engineering from Kyiv Polytechnical Institute in 2005. Recognized for his long-standing collaboration to the work of the Association, Dr. Agamalov has been honored with the title of Distinguished Member of CIGRE in 2016. Now he is working as an independent researcher for clean and efficient energy sources.

Research Field

Oleg Agamalov: power and energy systems, control systems, plasma physics, applications of magnetic reconnection.